Molecular Composition of Particulate Matter Emissions from Dung and Brushwood Burning Household Cookstoves in Haryana, India

Lauren T. Fleming[1], Peng Lin[2], Alexander Laskin[2], Julia Laskin[2], Robert Weltman[3], Rufus D. Edwards[3], Narendra K. Arora[4], Ankit Yadav[4], Simone Meinardi[1], Donald R. Blake[1], Ajay Pillarisetti[5],
5   Kirk R. Smith[5], Sergey A. Nizkorodov[1]

[1]Department of Chemistry and [3]Department of Epidemiology, University of California, Irvine, CA 92617
[2]Department of Chemistry, Purdue University, West Lafayette, IN 47907
[4]The Inclen Trust, Okhla Industrial Area, Phase-I, New Delhi-110020, India
[5]School of Public Health, University of California, Berkeley, CA 94720

10   *Correspondence to*: Rufus D. Edwards (edwardsr@uci.edu) and Sergey A. Nizkorodov (nizkorod@uci.edu)

Abstract. Emissions of airborne particles from biomass burning are a significant source of black carbon (BC) and brown carbon (BrC) in rural areas of developing countries where biomass is the predominant energy source for cooking and heating. This study explores the molecular composition of organic aerosols from household cooking emissions with a focus on identifying fuel-specific compounds and BrC chromophores. Traditional meals were prepared by a local cook with dung
15   and brushwood-fueled cookstoves in a village in Palwal district, Haryana, India. Cooking was done in a village kitchen while controlling for variables including stove type, fuel moisture, and meal. Fine particulate matter ($PM_{2.5}$) emissions were collected on filters, and then analyzed via nanospray desorption electrospray ionization/high resolution mass spectrometry (nano-DESI-HRMS) and high performance liquid chromatography/photodiode array/high resolution mass spectrometry (HPLC-PDA-HRMS) techniques. The nano-DESI-HRMS analysis provided an inventory of numerous compounds present in
20   the particle phase. Although several compounds observed in this study have been previously characterized using gas chromatography methods, a majority of the species in the nano-DESI spectra were newly observed biomass-burning compounds. Both the stove (*chulha* or *angithi*) and the fuel (brushwood or dung) affected the composition of organic aerosols. The geometric mean of the $PM_{2.5}$ emission factor and the observed molecular complexity increased in the following order: brushwood/*chulha* (7.3±1.8 g kg^{-1} dry fuel, 93 compounds), dung/*chulha* (21.1±4.2 g kg^{-1} dry fuel, 212 compounds),
25   and dung/*angithi* (29.8±11.5 g kg^{-1} dry fuel, 262 compounds). The mass-normalized absorption coefficient (MAC_{bulk}) for the organic-solvent extractable material for brushwood $PM_{2.5}$ was 3.7±1.5 m^2 g^{-1} and 1.9±0.8 m^2 g^{-1} at 360 nm and 405 nm, respectively, which was approximately a factor of two higher than that for dung $PM_{2.5}$. The HPLC-PDA-HRMS analysis showed that, regardless of fuel type, the main chromophores were $C_xH_yO_z$ lignin fragments. The main chromophores accounting for the higher MAC_{bulk} values of brushwood $PM_{2.5}$ were $C_8H_{10}O_3$ (tentatively assigned to syringol), nitrophenols
30    $C_8H_9NO_4$, and $C_{10}H_{10}O_3$ (tentatively assigned to methoxycinnamic acid).

1 Introduction

Approximately 3 billion people live in residences where solid fuels (coal, wood, charcoal, dung, and crop residues) are combusted for cooking (Smith et al., 2014). Approximately 57% of Indian households report use of wood (49%) or crop residues (9%) as their primary cookfuels, while 8% report dung as a primary cookfuel (Census of India, 2011). However, many households will routinely use two or more of these fuels in combination for their cooking needs in simple, home-made traditional stoves, or *chulhas*. These biomass-burning cookstoves have low combustion efficiencies and produce significant emissions of pollutants, including fine particulate matter ($PM_{2.5}$).

Epidemiological literature statistically links household air pollution from solid biomass combustion to acute lower respiratory infections in children, heart disease, stroke, cataracts, cancers in adults, and low birth weight for infants of women exposed during pregnancy (Smith et al., 2014). $PM_{2.5}$ are small enough to infiltrate deep into the lungs and penetrate the body's defenses, and therefore $PM_{2.5}$ exposure has been commonly used for estimating risks from both ambient air pollution and cigarette smoke (Finlayson-Pitts and Pitts, 2000). The degree of adverse health effects of cookstove smoke likely depends on the chemical composition of the $PM_{2.5}$, however, the exact relationship between the chemical composition and health effects is largely unknown (Araujo et al., 2008).

Household cooking is estimated to be responsible for 26-50% of ambient $PM_{2.5}$ in India (Chafe et al., 2014; Guttikunda et al., 2016; Lelieveld et al., 2015). In this emissions mixture, carbonaceous particles affect climate directly by scattering and absorbing incoming solar radiation and indirectly by acting as cloud condensation nuclei (Crutzen and Andreae, 1990). In addition to black carbon (BC), which absorbs solar radiation across the entire visible spectrum, some molecules in biomass burning organic aerosols (BBOA) efficiently absorb blue and near-UV solar radiation resulting in classification of BBOA as brown carbon (BrC) (Laskin et al., 2015). Modeling studies have shown that in certain geographic areas climate warming by BrC has the potential to outweigh cooling by scattering organic aerosols (Feng et al., 2013). South Asia has been identified as one of these unique regions where emissions from cookstoves are a significant source of regional BrC (Feng et al., 2013). Cookstove emissions have been studied in both the laboratory and field settings. Field studies typically involve observations and measurements during daily cooking activities in rural village homes. For example, Xiao et al., (2015) measured BC and $PM_{2.5}$ throughout the day for 6 different houses to monitor indoor concentrations in the household. In the laboratory, water boiling test (WBT) protocols are utilized to evaluate stove performance (Global Alliance for Clean Cookstoves, 2014). The WBT standard protocols are made up of three phases to represent the stove's combustion efficiency while cooking: (1) high power, cold start (2) high power, hot start (3) low power, simmer (Global Alliance for Clean Cookstoves, 2014). While the WBTs can be carried out under more controlled conditions, recent studies have found that the WBTs fail to capture periods of low combustion efficiency in cooking events (Chen et al., 2012; Johnson et al., 2008, 2009). This is due to daily cooking activities involving more than just boiling water (Johnson et al., 2009). Some cooking techniques require a smoldering fire, for example, the cooking of *chapatti,* a traditional Indian flat bread (Johnson et al., 2009). Alternately, these low combustion efficiency periods may be a consequence of multitasking around the home (Johnson et al., 2009). The literature estimates

that emissions of $PM_{2.5}$ (Roden et al., 2009) and CO/CO_2 ratios (Johnson et al., 2008; Kituyi et al., 2001; Ludwig et al., 2003) are underrepresented by the WBTs relative to field measurements by a factor of 3. There are also concerns that WBTs cannot be scaled to real cooking events and that climate models may underrepresent global emissions from biomass-burning cookstoves (Chen et al., 2012; Johnson et al., 2008, 2009).

5   A number of studies have characterized optical properties of cookstove BBOA. Depending on the measurement approach different metrics of aerosol absorption have been reported. In general, methods that do direct measurements on aerosol particles without extraction report mass-normalized absorption cross section of aerosols ($MAC_{aerosol}$). Absorption measurements with the extracted material report mass-normalized absorption cross section of bulk material (MAC_{bulk}). In this paper, we use subscript "bulk" to help minimize confusion between MAC_{bulk} and $MAC_{aerosol}$. The two can be related if

10   the particle size distribution is known (Laskin et al., 2015). An advantage of MAC_{bulk} is that it can be used to calculate the imaginary refractive index of the organic material (Laskin et al., 2015). For particles that are made of material with a real refractive index of 1.5 and that are small in diameter relative to the wavelength, $MAC_{aerosol} \sim 0.7 \times MAC_{bulk}$ (Laskin et al., 2015).

    Stockwell et al., 2016 utilized photoacoustic extinctiometers (PAX) to conduct in situ absorption measurements at 405 and

15   870 nm, resulting in particle absorption coefficients from cookfire emissions in Nepal. With a literature-recommended mass absorption coefficient for light-absorbing organic compounds (Lack and Langridge, 2013) and the measured aerosol absorption by PAX, they approximated particle absorption emission factors (EFs) due to the light-absorbing organic compounds in particles. OC absorption EFs were 1.5 times higher for the hardwood smoke (EF=8.40 g kg^{-1} fuel) compared to the dung smoke (EF=5.43 g kg^{-1} fuel). Pandey et al., 2016 collected $PM_{2.5}$ on filters from cookfires in India, fueled by

20   wood, agricultural residues, dung, and a mixture thereof and reported $MAC_{aerosol}$ values. They found that the $MAC_{aerosol}$ at 550 nm was a factor of 2.6 higher for fuel wood (1.3 m^2 g^{-1}) compared to dung (0.5 m^2 g^{-1}) (Pandey et al., 2016). This is consistent with Saleh et al., 2014, who found that for BBOA effective absorptivity of OA increases with BC to OA ratio. In Pandey et al., 2016, they measured EC/OC at 0.0649 for dung, and 0.0826 for fuel wood.

    Many organic components of BBOA have been successfully characterized in previous studies by electrospray ionization high

25   resolution mass spectrometry (ESI-HRMS) (Budisulistiorini et al., 2017; Laskin et al., 2009; Lin et al., 2012, 2016, 2017; Smith et al., 2009; Wang et al., 2017; Willoughby et al., 2016). For example, ESI-HRMS was used to analyze the particle-phase organic constituents of smoke samples collected during the Fire Lab at Missoula Experiment (FLAME) campaign (Laskin et al., 2009; Smith et al., 2009). Fuels utilized in the FLAME studies were selected to represent North American wild fires and the publications focused on non-woody biomass fuels such as detritus and litter as well as *ceanothus* from the US

30   Pacific Northwest. Smith et al., 2009 reported an inventory of species in particle-phase BBOA, with 70% of the compounds being reported for the first time. Laskin et al., 2009 examined the nitrogen-containing species and observed that a large fraction of the detected species were N-heterocyclic compounds. Lin et al., 2016 identifies fuel-specific BrC chromophores in particles collected from the FLAME-4 experiments via high performance liquid chromatography/photodiode array/high resolution mass spectrometry (HPLC-PDA-HRMS). Two of the four fuels were woody biomass specific to North America.

They found that nitroaromatics, PAHs, and polyphenols were responsible for the light absorption by BBOA (Lin et al., 2016). Recent papers investigated the chromophores in BBOA from Lag Ba'Omer, a nationwide bonfire festival in Israel (Bluvshtein et al., 2017; Lin et al., 2017). They found nitroaromatics to be the most prominent chromophores in these samples. Budisulistiorini et al. 2017 similarly identified 41 chromophores from Indonesian peat, charcoal, and fern/leaf

5   burning with a method relying on chromatographic separation and simultaneous detection by spectrophotometry and ESI-MS. They identified three types of chromophores: oxygenated, nitroaromatics, or sulfur-containing (Budisulistiorini et al., 2017).

The goal of the current study is to understand the composition of cookstove BBOA in additional detail than afforded by previous measurements. We do this by 1) generating and collecting BBOA from prescribed cooking events carried out by a

10   local cook and 2) using high-resolution mass spectrometry techniques to characterize their particle-phase composition. This is part of a larger study attempting to document the contribution of household solid fuel combustion to air pollution in India. In this paper we provide an inventory of particle-phase compounds produced from actual cooking events detected by nano-DESI-HRMS and an assessment of BrC chromophores specific to the biomass type used based on HPLC-PDA-HRMS analysis. In addition, we compare particle-phase constituents in cookfire smoke produced from different traditional stoves

15   and fuels.

2 Experimental Methods

2.1 Field site

This study was conducted at the SOMAARTH Demographic, Development, and Environmental Surveillance Site (Balakrishnan et al., 2015; Mukhopadhyay et al., 2012; Pillarisetti et al., 2014) run by the International Clinical

20   Epidemiological Network (INCLEN) in Palwal District, located approximately 80 km south of New Delhi. SOMAARTH covers 51 villages across three administrative blocks, with an approximate population of 200,000. Palwal District has a population of approximately 1 million over ~1400 km^2; 39% of households in the district utilize wood as their primary cookfuel, followed by dung (25%) and crop residues (7%) (Census of India, 2011).

2.2 Sample collection

25   Over 34 days in August-September 2015, PM$_{2.5}$ samples were collected from a kitchen in the village of Khatela, Palwal, Haryana, India. Figure 1 shows (A) the kitchen setup and (B) the stoves (*angithi* and *chulha*) and fuels (dung and brushwood) used. The stoves and fuels were obtained locally and traditional meals were prepared by a local cook. The cook was instructed by the experimenters to prepare a particular, standard meal using the selected fuel and stove. All *angithi* cookstoves burned dung and were used to prepare buffalo fodder. *Chulha* cookstoves burned either brushwood or dung fuels

30   and were used to prepare a traditional meal of *chapati* and vegetables for 4 people. Vegetables were cooked in a pressure

cooker that rests on top of the *chulha* (Figure 1B). *Chapatti* were cooked in the air space next to the fuel, as is typical for this area. Brushwood/*angithi* cookfires were never tested because this combination is not frequently used in the local households. Figure S2.1 shows a diagram of sample collection. $PM_{2.5}$ emissions were sampled via three-pronged probes that hung above the cookstove. Air sampling pumps (PCXR-8, SKC Inc.) created a flow of BBOA emissions through aluminum tubing

5   during cooking events. BBOA was captured through cyclone fractionators (2.5 μm cut point, URG Corporation) and the resultant flow was taken through a stainless steel filter holder containing a PTFE filter (Teflon B, SKC Inc., 47 mm). One filter was collected for chemical analysis (Teflon B), and another filter for gravimetric analysis (Teflon A). Flows were measured via a mass flowmeter (TSI 4140) before and after each cooking event to ensure it had not varied more than 10%. The pumps were turned on before cooking began so that emissions from the entire cooking event were captured and turned

10 off when the fire was out. Stove dimensions and their distance from the probe inlets are detailed in Figure S3.1. Prior to analysis, filters were stored in petri dish slides at -80°C other than during transportation and use. This includes time at the field site (1-6 hours) and transportation back to the United States (24 hours). During these times, samples were stored at ambient temperature.

2.3 Nano-DESI-HRMS analysis

15 $PM_{2.5}$ collected on PTFE filters were analyzed with an LTQ-Orbitrap^{TM} high resolution mass spectrometer (ThermoFisher Scientific) equipped with a custom built nano-DESI source (Roach et al., 2010a, 2010b). Nano-DESI consists of two electrified capillaries with a small (< 1 mm) droplet, or solvent bridge, forming at the point of their contact. The nano-DESI solvent mixture (70% CH_3CN/30% H_2O, optimized for the stability of the nano-DESI source) flows through an electrified capillary at a flow rate of 0.3-1 μL/min. The droplet is lowered to the substrate's surface where the analyzed material is

20 extracted by the solvent and immediately sprayed in the mass spectrometer inlet. It has been shown that the nano-DESI dissolves all extractable material on the filter surface (Roach et al., 2010a, 2010b). To ensure the material on the filter is not depleted the droplet is moved across the filter's surface at roughly 0.2 cm/min. The spray voltage was 3.5 kV and the instrument was operated in positive ion mode. The mass accuracy of the HRMS was calibrated over a wide *m/z* range with a ThermoFisher Scientific standard calibration mixture. Two separate mass spectra were obtained from different portions of

25 the filter to ensure reproducibility. Only peaks that showed up in both spectra were retained for further analysis. Peaks with signal-to-noise ratios of greater than 3 were extracted from the time-integrated nano-DESI chromatograms using Decon2LS software. Peaks containing ^{13}C isotopes were excluded from analysis. Sample and solvent-blank mass spectra peaks were clustered with a tolerance of 0.001 *m/z* using a second-order Kendrick analysis with CH_2 and H_2 base units (Roach et al., 2011). The spectra were internally mass-calibrated by assigning prominent peaks of common BBOA

30 compounds first, and fitting the observed-exact *m/z* deviation to a linear regression curve. The *m/z* correction introduced by the internal calibration was <0.001 *m/z* units, but even at these small levels the correction helped reduce the ambiguity in the assignments of unknown peaks. We focused on analyzing peaks with *m/z*< 350, as peaks above this *m/z* value were small in

abundance (on average 6% of total abundance), number of peaks (9% of the total number of peaks), and in many cases could not be assigned unambiguously. Exact masses were assigned using the freeware program Formula Calculator v1.1 (http://magnet.fsu.edu/~midas/download.html). The permitted elements and their maximal numbers of atoms were as follows: C (40), H (80), O (35), N (5), and Na (1). Peaks that could not be assigned within the described parameters had

5   small abundances and were not pursued further. There were a few notable exceptions, namely, the potassium salt peaks discussed below. Conversely, potassium-organic adducts were not observed presumably due to the higher affinity of organic molecules to Na^+ compared to K^+. Permitting sulfur, chloride, and phosphorus did not increase the fractions of assignable peaks, nor did it change the assignments for the peaks we report. The double-bond equivalent (DBE) values of the neutral formulas were calculated using the equation: DBE = C - H/2 + N/2 + 1, where C, H, and N correspond to the number of

10 carbon, hydrogen, and nitrogen atoms, respectively.

2.4 HPLC-PDA-HRMS

The samples were further analyzed with an HPLC-PDA-HRMS platform (Lin et al., 2016). To prepare the samples for analysis half of the PTFE filter was extracted overnight in mixture of acetonitrile, dichloromethane, and hexane solvents (2:2:1 by volume, 5 mL total), which was empirically found to work well for extracting a broad range of BBOA compounds

15 (Lin et al., 2017). The solutions were then filtered with PVDF filter syringes to remove insoluble particles (Millipore, Duropore, 13mm, 0.22 µm). The solutions were concentrated under N_2 flow, and then diluted with water and dimethyl sulfoxide (DMSO) to a final volume around 150 µL. The separation was performed on a reverse-phase column (Luna C18, 2 x 150 mm, 5 µm particles, 100 Å pores, Phenomenex, Inc.). The mobile phase comprised of 0.05% formic acid in LC/MS grade acetonitrile (B) and 0.05% formic acid in LC/MS grade water (A). Gradient elution was performed by the A/B mixture

20 at a flow rate of 200 µL/min: from 0-3 min hold at 90% A, 3-62 min linear gradient to10% A, 63-75 min hold at 10% A, 76-89 min linear gradient to 0% A, 90-100 min hold at 0% A, then 101-120 min hold at 90% A. The ESI settings were as follows: 5 µL injection volume, 4.0 kV spray potential, 35 units of sheath gas flow, 10 units of auxiliary gas flow, and 8 units of sweep gas flow. The solutions were analyzed in both positive and negative ion ESI/HRMS modes.

The HPLC-PDA-HRMS data were acquired and first analyzed using Xcalibur 2.4 software (Thermo Scientific). Possible

25 exact masses were identified by LC retention time using the open source software toolbox MZmine version 2.23 (http://mzmine.github.io/) (Pluskal et al., 2010). Formula assignments were obtained from their exact *m/z* values using the Formula Calculator v1.1.

2.5 MAC_bulk and AAE

Selected filter halves were extracted as described in section 2.4. Absorption spectra of the extracts were collected with a

30 dual-beam UV-Vis spectrophotometer (Shimadzu UV-2450). MAC_bulk values were calculated from the following equation:

$$MAC_{bulk}(\lambda) = \frac{A_{10}(\lambda) \cdot \ln(10)}{b \cdot C_{mass}}$$ (1)

where A_{10} is the base-10 absorbance, b is the path length of the cuvette (m), and C_{mass} is the mass concentration of the extracted organic material in (g m^{-3}). The largest uncertainty in MAC_{bulk} came from uncertainty in C_{mass} of the extract. First, the overall mass of $PM_{2.5}$ on the filter had to be estimated from another filter collected specifically for gravimetric analysis. The $PM_{2.5}$ mass on the chemical analysis filter was calculated from the mass on the gravimetric analysis filter after accounting for different flows through the two filters (See Figure S2.1). This calculation assumed the same $PM_{2.5}$ collection efficiency for both filters. The particle mass distribution on the filter was assumed to be uniform, and the extraction efficiency of $PM_{2.5}$ mass was estimated to be 50% by comparing the weights of filters before and after the extraction. Uncertainties incorporate flow rate measurements (10% relative error) and extraction efficiency of $PM_{2.5}$ mass (40% relative error). Absorption angstrom exponents (AAE) were calculated for both samples by fitting the log(MAC_{bulk}) vs. log(λ) to a linear function over the wavelength range of 300 to 700 nm. It should be noted that there are many methods for measuring optical properties of $PM_{2.5}$ particles, and the method used here provides MAC_{bulk} and AAE of extractable organic bulk material. The advantages and limitations of other methods are explained in Laskin et al., 2015.

3 Results and Discussion

3.1 Nano-DESI-HRMS analysis of cookstove particles

Representative nano-DESI mass spectra from the three major types of cookfires sampled are shown in Figure 2. It is clear from the mass spectra in Figure 2 that the three combinations of fuel/stove types lead to distinct particle compositions. We compare the particle composition of the three major cookfire types by averaging the percentage of $C_xH_yN_w$, $C_xH_yO_z$, and $C_xH_yO_zN_w$ peaks in the nano-DESI spectra from multiple samples. Samples used and a summary of the following discussion is detailed in Table S1.1. The overwhelming majority of detected species by nano-DESI in dung cookfire smoke $PM_{2.5}$ was attributed to $C_xH_yN_w$, compounds that contain only carbon, hydrogen, and nitrogen atoms. The average count-based fractions from $C_xH_yN_w$ species were 79.9%±4.4% and 82.1%±1.0% for dung/*chulha* and dung/*angithi* experiments, respectively, but only 23.8%±7.8% for brushwood/*chulha* experiments. All nitrogen-containing compounds in the smoke $PM_{2.5}$ come from the nitrogen content in the fuels (Coggon et al., 2016) which is likely higher for dung. Stockwell et al. 2016 reported the nitrogen content of yak dung as 1.9% by weight, while it is found to be lower for woods such as black spruce (0.66% by wt) and ponderosa pine (1.09% by wt) (Hatch et al., 2015). It should be noted that another study of fuels in India found the nitrogen content was roughly the same for brushwood (1.4±0.3% by wt) and dung (1.4±0.1% by wt) (Gautam et al., 2016), so additional characterization of fuel composition in the future is desirable. In contrast to dung fuel, $PM_{2.5}$ from brushwood cookfire smoke contained higher fractions of $C_xH_yO_z$ species. Specifically, the count-based fraction assigned as $C_xH_yO_z$ species was 43.1%±14.6% in brushwood/*chulha* cookfires compared to only 4.1%±0.9% and 3.2%±3.3% for dung/*chulha*

and dung/*angithi* experiments, respectively. Many of the $C_xH_yO_z$ formulas were consistent with species reported previously as lignin-pyrolysis products (Collard and Blin, 2014; Simoneit et al., 1993). Fractions of $C_xH_yO_zN_w$ did not correlate well with fuel/stove variables and ranged from 4.1% to 34.4% in the analyzed samples.

Potassium (Hosseini et al., 2013; Sullivan et al., 2014) and levoglucosan (Jayarathne et al., 2017; Simoneit et al., 1999) are well-established flaming and smoldering BB tracers, respectively. Gas-phase chlorine species have been observed in BBOA previously (Lobert et al., 1999; Stockwell et al., 2016). Therefore it is not surprising that inorganic salt peaks containing potassium and chlorine were observed in more than half of dung cookfires (8 out of 14) and all brushwood cookfires. These peaks were pursued apart from the original analysis because the peak abundance was very large in many mass spectra, and they served as convenient internal *m/z* calibration points. These mass spectra all contained K_2Cl^+ as the most prominent salt peak and $K_3Cl_2^+$ was also present in a few mass spectra. Isotopic variants of these salts, namely with either ^{37}Cl or ^{41}K (24% or 6.7% natural abundance) instead of ^{35}Cl or ^{39}K (76% or 93.3% natural abundance), were also found. The resolving power of the HRMS instrument is insufficient to distinguish the isotopic shifts from Cl and K (Δ mass$_{37Cl-35Cl}$= 1.997 Da, Δ mass$_{41K-39K}$= 1.998 Da) but one or both of the isotopes were consistently present in all mass spectra containing potassium ions. Adducts corresponding to a replacement of K by Na were also detected. The observed potassium signals may have depended not only on the potassium content of the fuel but also on the amount of flaming combustion (combustion efficiency), the specific food items cooked, or the stove material itself. Inorganic salts were observed in all *chulha* cookfire $PM_{2.5}$ samples regardless of fuel type and were absent in all *angithi* cookfire $PM_{2.5}$ samples. On average, chulha stoves have a higher combustion efficiency (dung/*chulha* 90.7% ± 0.6%, dung/*angithi* 87.5% ± 1.8%) consistent with more flaming combustion and therefore more potassium emissions. The *chulha* and *angithi* stoves produced meals for people or animal fodder, respectively. Also, the *chulha* was made mainly from brick with a local covering of local clay, whereas the *angithi* only from clay. With the presently available data it is impossible to determine whether the potassium salts originated from flaming combustion, from the *chulha* material, or is the result of different food items cooked.

Levoglucosan was present in 3 out of 8 dung/*chulha* cookfires, 4 out of 6 dung/*angithi* cookfires, and 4 out of 11 brushwood/*chulha* cookfires. We expect levoglucosan to be found in BBOA from all fires based on other studies (Jayarathne et al., 2017), and we therefore conclude that levoglucosan peak must have been suppressed in the nano-DESI source by the more ionizable components of the mixture. By extension of the same logic, ions corresponding to other carbohydrates, and more broadly to lignin-derived CHO species, were likely suppressed by this technique, and therefore a significant fraction of BBOA constituents may be absent in this inventory. Due to the variability in observing levoglucosan we conclude that for ESI-MS studies levoglucosan serves as a marker rather than a tracer for digested biomass burning and woody biomass burning.

3.2 Particle-phase biomass burning markers

An inventory of compounds that were reproducibly observed in samples from three different cooking events using the same fuel/stove combination was compiled. Samples were chosen for the inventory considering the measured fuel moisture content and meal cooked, with the goal of comparing samples from similar cookfires (see SI Table S1.1 for sample details). Peaks that did not appear in mass spectra of all three samples were discarded to ensure reproducibility and help filter out

5   noise peaks from the nano-DESI source. The remaining peak abundances were first normalized to the largest peak abundance then the three mass spectra were averaged. Since the absolute peak abundances varied in individual spectra, only approximate relative abundances are reported here grouped into three logarithmic bins, denoted as LOW (<1%), MEDIUM (1-9.99%), HIGH (10-100%). This analysis was completed for the emissions from each of the three types of cookstove-fuel combinations studied in this work.

10   Figure 3 summarizes how reproducibly-detected $PM_{2.5}$ compounds are organized in the inventory. First, we provide a list of compounds common to the emissions from all 3 types of cookfires including: dung/*chulha*, dung/*angithi*, and brushwood/*chulha* (Section 3.3, Table 1). Then, we discuss compounds exclusively found in the brushwood/*chulha* cookfire emissions (Section 3.4, Table S4.1). Within section 3.5 we discuss compounds unique to the dung/*chulha* (Table S4.2) and the dung/*angithi* (Table S4.3) cookfire experiments, as well as the compounds they had in common (Table 2).

15   The numbers of reproducibly-detected formulas are shown in Figure 3 in blue. $PM_{2.5}$ from dung cookfires had a higher observed chemical complexity (i.e., had more observed peaks) than $PM_{2.5}$ from brushwood cookfires. Further, there were more observed peaks in $PM_{2.5}$ from dung/*angithi* cookfires compared to dung/*chulha* cookfires. There were 93 compounds reproducibly detected in the brushwood/*chulha* cookfire $PM_{2.5}$ samples compared to 212 and 262 for dung/*chulha* and dung/*angithi* cookfires, respectively. There were five compounds the *chulha* cookfires had in common, with two of them being the potassium salt peaks described earlier. There was one compound ($C_{14}H_{16}O_3$) shared by only dung/*angithi* and

20   brushwood/*chulha*. Because of the small number of these peaks, they will not be discussed in this paper. In the following sections, we discuss compounds that are common in all cookfires, as well as unique compounds.

Figure 4 summarizes the BBOA inventory described in more detail in sections 3.3-3.5, i.e., compounds common to dung/*chulha*, dung/*angithi*, brushwood/*chulha* cookfires; compounds found exclusively in the emissions from

25   brushwood/*chulha* cookfires; and species that are unique to dung cookfires. Figure 4A compares the fraction of count-based, normalized abundance in each elemental category. $PM_{2.5}$ compounds shared among all samples of this study are diverse. In terms of count-based abundance, compounds emitted from all dung-burning cookfires are largely nitrogen-containing. From Figure 4B, the common compounds make up the vast majority (97%) of detected compounds from the brushwood/*chulha* cookfires. Similarly for the dung cookfires, the common cookfire compounds (grey) and dung cookfire compounds (brown)

30   make up 95% or more of the mass spectra abundance as shown in Figure 4B. Therefore, the common compounds (Table 1) and dung compounds inventories (Table 2) contain the bulk of the $PM_{2.5}$ species in terms of count-based abundance.

3.3 Compounds common to dung/*chulha*, dung/*angithi*, brushwood/*chulha* cookfires

Table 1 provides a complete list of eighty reproducibly-detected compounds that were common to emissions from all cookfires. These common compounds make a large contribution to the mass spectra for every cookfire type (Figure 4), with MEDIUM being the most common relative abundance given in Table 1. More than half of the abundance (59%) was due to the nitrogen-containing compounds ($C_xH_yN_w$ or $C_xH_yO_zN_w$), as shown in Figure 4a. ESI detection likely biases the elemental

5   make up of smoke $PM_{2.5}$, as nitrogen-containing species are more easily ionized compared to sugars and lignin-derived compounds (Laskin et al., 2010; Wan and Yu, 2006). Nevertheless, a large overlap in the $C_xH_yN_w$ and $C_xH_yO_zN_w$ species was observed.

The common compounds make up a large fraction for all cookfire types. This is especially true for the sample from brushwood/*chulha* cookfires where their fraction is ~86% in number. Many of these $C_xH_yO_z$ species have elemental formulas

10   consistent with typical lignin and cellulose-derived products such as anisaldehyde, veratraldehyde, vinylguaiacol, syringylethanone, trimethoxyphenylethanone, etc. reported previously in the literature (Laskin et al., 2009; Simoneit et al., 1993; Smith et al., 2009). These tentative molecular assignments are listed in Table 1 alongside their elemental formulas. Approximately 20% of the common compounds (17 out of 80 formulas) have been also identified in earlier studies reporting molecular characterization of $PM_{2.5}$ samples collected from burning of one or more of the following fuels: Alaskan duff,

15   ponderosa pine duff, southern United States pine needles, or ceanothus fuels (Laskin et al., 2009; Smith et al., 2009). Many of these fuels are non-woody and all are undigested biomass, very different kinds of biomass from those used as cookstove fuels in this study and in this region of India. This suggests that perhaps 20% of the compounds listed in Table 1 might be reproducibly detected in BBOA samples using ESI-MS regardless of biomass type. The overlap is not surprising as all biomass is composed of three polymers: lignin, hemicellulose, and cellulose (Collard and Blin, 2014).

20   **3.4 Compounds found exclusively in the emissions from brushwood/*chulha* cookfires**

Table S4.1 lists the compounds observed exclusively in the samples from brushwood/*chulha* cookfires. Many of them correspond to lignin-derived products that have been previously identified in BBOA by gas chromatography methods, as indicated in Table S4.1 (Lee et al., 2005; Simoneit, 2002; Simoneit et al., 1993; Smith et al., 2009). Lignin is an essential component of wood comprising roughly a third of its dry mass (Collard and Blin, 2014; Simoneit, 2002). Lignin is generally

25   composed of *p*-coumaryl, coniferyl, and syringyl alcohol units. During pyrolysis, the coumaryl, vanillyl, and syringyl moieties, respectively, are preserved and are found in smoke. More generally, the lignin pyrolysis products found in smoke contain a benzene ring often with hydroxy and/or methoxy substituents. Based on these previous observations, and the assumption that these are lignin pyrolysis products, tentative molecular structures were assigned to $C_xH_yO_z$ compounds. It is likely that some $C_xH_yO_z$ molecular species specific to the emissions from the brushwood burning were not detected in this

30   study due to their low ionization efficiency.

3.5 Species unique to dung smoke $PM_{2.5}$

Overall, the chemical composition of $PM_{2.5}$ samples of dung-burning emissions was observed to be far more complex than the samples from the brushwood-burning cookfires. Table 2 lists the 115 compounds found exclusively and reproducibly in the dung-fueled samples. These compounds are largely $C_xH_yN_w$, as shown in Figure 4b. Only a few of the elemental formulas, $C_8H_{16}N_2$, $C_{11}H_8N_2$, and $C_{13}H_{11}ON$, have been reported previously (Laskin et al., 2009; Smith et al., 2009).

5   In addition to the common dung compounds listed in Table 2, there were compounds detected exclusively in the emissions from either dung/*chulha* cookfires (Table S4.2) or dung/*angithi* cookfires (Table S4.3). All of these compounds are nitrogen-containing, and none have been reported previously as BBOA compounds, to the best of our knowledge. However, in this section, we combine all compounds found in dung-burning cookfire $PM_{2.5}$, presented in Tables 2, S4.2, and S4.3, and discuss their possible molecular character.

10   Figure 5 shows the double bond equivalent (DBE) as a function of the carbon number of compounds detected in all investigated samples. The DBE versus C dependence for classes of compounds with different degrees of unsaturation, including: terpenes (red), polyenes (orange), polycyclic aromatic hydrocarbons (yellow shaded, PAHs) are also shown to aid the classification of the compounds observed in the $PM_{2.5}$ samples. Thirty of the 193 formulas fall in the PAH region of the plot suggesting that they have aromatic structures (Figure 5a). Figure 5b compares the DBE values of the molecular

15   components detected in the emissions exclusive to brushwood/*chulha* cookfires (Table S4.1) and the common compounds from all studied samples (Table 1). In general, the DBE increases with carbon number for the compounds common to all cookfires. Only eight of the 87 compounds fall directly in the PAH region. There are more aromatic structures specific to the dung smoke compared to the compounds detected in all cookfires.

Detected nitrogen compounds with high DBE values are likely N-heterocyclic PAH compounds. Figure 6 displays possible

20   structures for the select detected nitrogen-containing compounds with a high DBE. Purcell et al. (2007) found that pyridinic PAH compounds were readily ionized from standard mixtures of N-heterocyclics in positive-ion ESI. This gives us more confidence in our observation of $C_{13}H_9N$, tentatively acridine, and $C_{11}H_8N_2$, tentatively β-carboline, which have pyridinic nitrogen atoms and likely have high ionization efficiencies. The peak abundances of these compounds are significant, with medium and high designations, respectively. $C_{12}H_9ON$ cannot have a pyridinic nitrogen and is tentatively assigned as

25   phenoxazine.

Kendrick analysis identifies homologous series of structurally-related compounds that share a core formula and differ in the number (n) of additional CH_2 units (Hughey et al., 2001). 172 of the 193 detected compounds from the dung-burning cookfire emissions can be grouped into 43 homologous series based on the Kendrick mass defect plot, as shown in Figure 7. There are 15 homologous series and 5 independent formulas that make up the 61 total $C_xH_yN_w$ (red) compounds. This

30   suggests that there are at least 20 distinct types of structures that made up the observed $C_xH_yN_w$ species. Similarly, there are 30 homologous series for $C_xH_yO_zN_w$ (purple) formulas and 12 $C_xH_yO_zN_w$ formulas yielding at least 42 distinct types of structures for this formula category. There are no homologous series from $C_xH_yO_z$ species, presumably because only a few members of this group can be detected by ESI-based methods in the $PM_{2.5}$ from the dung cookfires. From this analysis, there are at least 66 unique types of structures from the 193 compounds detected from dung-burning cookfire emissions. This

Kendrick analysis suggests that some of the observed N-heterocyclic PAHs have alkyl substituents. For example, phenoxazine and β-carboline (Figure 6) serve as the core molecules in the homologous series $C_nH_{2n-15}ON$ and $C_nH_{2n-14}N_2$, respectively (Figure 7).

3.6 Light-absorbing properties and chromophores from cookstove emissions

5   Figure 8 show MAC_{bulk} values, which represent bulk absorption coefficient normalized by mass concentration of organic solvent extractable components. The MAC_{bulk} values were determined assuming that 50 percent of the particle mass could be extracted from the filter. Error bars account for the uncertainties in the extraction efficiency (relative error 40%), and flows during sample collection (relative error 10%). MAC_{bulk} values for the samples from the brushwood burning are roughly twice that of dung between 300-580 nm. Assuming higher EC/OC for wood compared to dung as reported in Jayarathne et al.,

10 2017, the results are consistent with Saleh et al., 2014, who predict higher effective OA absorbance for higher BC to OA ratios.

MAC_{bulk} values at 400 nm were 1.9 ± 0.8 m^2 g^{-1} and 0.9 ± 0.4 m^2 g^{-1} for the samples from brushwood/*chulha* and dung/*chulha* cookfires, respectively. For comparison, Kirchstetter and colleagues reported MAC_{bulk} of 2.9 m^2 g^{-1} at 400 nm for the BrC in biomass smoke samples (Kirchstetter et al., 2004). Chen and Bond measured MAC_{bulk} values at 360 nm of nearly 2.0 m^2 g^{-1}

15 for methanol extracts of particles resulting from oak pyrolysis, and nearly 2.5 m^2 g^{-1} for pine wood pyrolysis (Chen and Bond, 2010). Our MAC_{bulk} value at 360 nm for brushwood was larger at 3.7 ± 1.5 m^2 g^{-1}, possibly due to a more efficient extraction of a broader range of chromophores by the solvents utilized. The pyrolysis temperature and wood composition could also contribute to the difference. Our MAC_{bulk} value at 360 nm for dung was lower compared to our brushwood sample at 1.8 ± 0.8 m^2 g^{-1}. This could be a combined result of the likely lower pyrolysis temperature and difference in the biomass

20 composition (Chen and Bond, 2010).

While the MAC_{bulk} values are smaller for the dung/*chulha* cookfires, the $PM_{2.5}$ emission factors (a detailed analysis of the emission factors will be reported in a follow up paper) are more than a factor of 2.5 higher for dung/*chulha* fires (21.1 ± 4.2 g kg^{-1} fuel) compared to brushwood/*chulha* fires (7.3 ± 1.8 g kg^{-1} fuel). The product $MAC_{bulk} \times EF$ can be used to estimate the contribution of smoke to the absorption coefficient for the per unit mass of the fuel burned. At 400 nm, $MAC_{bulk} \times EF =$

25 19.0 ± 9.2 m^2 kg^{-1} fuel and 13.9 ± 6.8 m^2 kg^{-1} fuel for dung/*chulha* fires and brushwood/*chulha* fires, respectively. For particles that are small in diameter relative to the wavelength, $MAC_{aerosol} \sim 0.7 \times MAC_{bulk}$ (Laskin et al., 2015). Based on this we can estimate $MAC_{aerosol} \times EF = 13.3\pm6.5$ m^2 kg^{-1} fuel and 9.7 ± 4.8 m^2 kg^{-1} fuel for dung/*chulha* fires and brushwood/*chulha* fires, respectively. The values are somewhat higher than the "EF B_{abs} 405 just BrC" values reported by Stockwell et al., 2016 at 405 nm, which were 8.40 m^2 kg^{-1} fuel and 5.43 m^2 kg^{-1} fuel for hardwood cooking smoke and dung cooking smoke,

30 respectively. However, both the present results and the data from Stockwell et al., (2016) show that the dung-based and wood-based fuels make comparable contributions to the absorption coefficient of the smoke for same amount of fuel consumed.

The AAE values for the extractable organics in brushwood and dung samples are 7.5 and 6.8, respectively. Our brushwood AAE fits into the lower end of the AAE range for extracted organics presented in Chen and Bond, 6.9 to 11.4 (Chen and Bond, 2010). Typical AAE values cited in the literature for BrC in BBOA are in a range of 2-11 (Kirchstetter et al., 2004; Laskin et al., 2015). The AAE of the entire cooking aerosol (with the contribution of the insoluble BC included) should be

5   lower. For example, Stockwell et al., 2016 reported in situ measurements of AAE of 3.01 and 4.63 for brushwood and dung cooking particles, respectively.

We now focus on identifying selected chromophores that contribute to the high MAC_{bulk} we observe for cookstove $PM_{2.5}$. Two cookfires using dung and brushwood fuels were selected for a more detailed analysis of the light-absorbing molecules (BrC chromophores). The dung cookfire utilized an *angithi* cookstove to prepare buffalo food. The brushwood cookfire was

10   used to prepare a traditional meal of rice and lentils with a *chulha*. More detailed sample information is provided in Table S1.3. The samples were analyzed using HPLC-PDA-ESI/HRMS platform following the methods described elsehwere (Lin et al., 2015, 2016, 2017). The identified chromophores and their PDA chromatograms are illustrated in Figure 9, and the retention times and peaks in the absorption spectra are listed in Tables 3 and 4 for the emissions from brushwood and dung cookfires, respectively.

15   The BrC chromophores for both brushwood and dung samples are largely $C_xH_yO_z$ compounds (Tables 3 and 4). We conclude that lignin-derived BrC chromophores account for the majority of the extracted light-absorbing compounds in both samples. We also found a few nitrogen-containing BrC chromophores (e.g., $C_9H_7NO_2$ and $C_8H_9NO_3$) in both the brushwood and dung samples. The woody and digested biomasses shared 3 strongly-absorbing chromophores, $C_8H_8O_4$ (tentatively vanillic acid), $C_{10}H_{12}O_3$ (tentatively ethyl methoxybenzoate), and $C_{13}H_{10}O_2$, as well as comparably weaker-absorbing chromophores.

20   $C_{10}H_{10}O_3$ is another strong absorber of near-UV radiation that was found in both samples. In the brushwood-derived $PM_{2.5}$, $C_{10}H_{10}O_3$ elutes at 18.3 min (λ_{max}= 337 nm), while in the dung smoke sample, it is not oberved until 24.5 min (λ_{max}= 299, 308 nm). These are clearly different chromophores with the same chemical formula, possibly coniferaldehyde and methoxycinnamic acid. $C_9H_8O_3$ is a similar case, in which the same chemical formula appears at different retention times in the selected ion chromatograms (SICs) for brushwood- and dung-derived $PM_{2.5}$. In the brushwood-derived $PM_{2.5}$ sample,

25   $C_9H_8O_3$ coelutes with $C_9H_7NO_2$ at 17.3 min (Table 3). In the dung $PM_{2.5}$ sample $C_9H_8O_3$ coelutes with $C_8H_8O_4$ and $C_9H_{10}O_4$ at 14.4 min (Table 4). The $C_9H_8O_3$ formula could correspond to coumaric acid for either retention time. Because the compound coelutes with other potential chromophores, we refrained from assigning a proposed structure to the chemical formula.

There were light-absorbing molecules specific to brushwood-derived $PM_{2.5}$ (Table 3) that could account for higher MAC_{bulk}

30   values compared to the dung-derived $PM_{2.5}$. $C_8H_9NO_4$ is a possible nitroaromatic compound with its absorbance peaking around 335 nm. $C_8H_{10}O_3$, tentatively syringol, is closely related to syringic acid, a lignin monomer. The formula was also detected in the dung-derived $PM_{2.5}$ sample, but the absorption was lower by approximately a factor of 20 and therefore is not considered a main chromophore.

There were strongly-absorbing BrC chromophores in the $PM_{2.5}$ generated by burning dung fuel that eluted in the first couple of minutes of the sample run (See Figure 9b). These early-eluting chromophores were likley polar compounds that were not retained well by the column and thus could not be assigned. The challenges with assigning co-eluting chromophores in BBOA were previously noted by Lin et al., 2016. For both $PM_{2.5}$ samples, most of the chromophores eluted in the first 30 minutes of the run shown in Figure 9. Compounds eluting in the range of 30 to 60 min were also satisfactorily separated, but these were weakly absorbing. The non-polar PAH compounds absorbing in UV-Vis range are not ionized by the ESI source and subsequently not detected by HRMS (Lin et al., 2016). It is possible that additional light-absorbing molecules essential to dung smoke were strongly retained by the column and eluted after 60 min.

Absorption spectra recorded in tandem with the mass spectra provide additional constraints on the assignments. For example, at 15.6 minutes $C_{10}H_{12}O_3$ and $C_9H_{10}O_3$ coeluted in both BBOA samples. These compounds were given the tentative assignments of ethyl-3-methoxybenzoate and veratraldehyde, respectively. The UV-Vis absorbance of ethyl-3-methoxybenzoate shown in Figure 10 provides a reasonable match for the recorded PDA spectra for both samples at a retention time of 15.6 min. Veratraldehyde, which is derived broadly from lignin, has an absoprtion spectrum that peaks at 308 nm in aqueous solution (Anastasio et al., 1997). Therefore, both ethyl-3-methoxybenzoate and veratraldehyde contribute to the spectrum observed by the PDA detector, although they cannot be completely separated with this HPLC protocol. For many formulas multiple structural isomers were observed in SICs with peaks appearing at more than one retention time. This behavior has been observed for other types of BBOA samples, described in Lin et al., 2016, and is inherent to lignin's nature such that a single $C_xH_yO_z$ chemical formula can correspond to multiple possible structural isomers. There are several cases in which chemical formulas show up multiple times in Tables 3-4. An example from the brushwood $PM_{2.5}$ (Table 3) is $C_9H_{10}O_4$ which elutes at 10.6 and 14.4 minutes. $C_9H_{10}O_4$ has been previously found in lignin pyrolysis BBOA in the forms of homovanillic acid and syringealdehyde (Simoneit et al., 1993). $C_8H_8O_4$ and $C_9H_{10}O_3$ are additional examples of the similar occurance in the sample of dung-derived $PM_{2.5}$, as they both appear twice in the SICs as shown in Table 4. One peak corresponding to $C_8H_8O_4$ is very likely vanillic acid (Simoneit, 2002; Simoneit et al., 1993). $C_9H_{10}O_3$ could be either veratraledehyde or homoanisic acid, both have been observed from lignin pyrolysis (Simoneit et al., 1993). Collectively, these results indicate that many of the lignin-like chromophores have multiple structural isomers, some of which have likely been observed before (Simoneit, 2002; Simoneit et al., 1993).

4 Summary

Molecular analysis of $PM_{2.5}$ emissions from three types of cookstove-fuel combinations showed that the observed chemical complexity of particle composition increased in the following order: brushwood/*chulha*, dung/*chulha*, dung/*angithi*. The compounds accounting for the additional complexity in dung-derived emissions were mostly $C_xH_yO_zN_w$ and $C_xH_yN_w$ species, which have not been identified before in cookstove BBOA. A substantial portion of the compounds specific to dung cookfires appeared to be aromatic based on their degree of unsaturation. The CH_2-Kendrick analysis of the nitrogen-

containing species from dung cookfires indicated that many may be structurally related by substitution with alkyl chains of variable length.

The estimated MAC_{bulk} values for the $PM_{2.5}$ emissions samples from brushwood/*chulha* and dung/*chulha* cookfires were comparable in magnitude and wavelength dependence to the values previously observed for BBOA samples. While the MAC_{bulk} values for the brushwood-derived BBOA were higher than those for the dung-derived BBOA, the particle emission factors had the opposite relationship. Therefore, per unit mass of burned fuel, the dung and brushwood fueled cookstoves may have comparable contribution to the overall light absorption. A set of $PM_{2.5}$ samples from brushwood/*chulha* and dung/*chulha* cookfires was analyzed using HPLC-PDA-HRMS to identify BrC chromophores. The vast majority of chromophores observed for both fuel types were lignin-like $C_xH_yO_z$ compounds. There were three retention times at which strongly-absorbing chromophores eluted for both samples: $C_8H_8O_4$ (vanillic acid), $C_{10}H_{12}O_3$ (methoxybenzoate), and $C_{13}H_{10}O_2$. There were also fuel-specific chromophores such as $C_{10}H_{10}O_3$ (distinct isomers for each fuel type), $C_8H_{10}O_3$ (syringol, brushwood), and $C_{12}H_{10}O_4$ (dung).

In this study, we characterized a wide range of particle-phase compounds produced by cookstoves, including the lignin-derived $C_xH_yO_z$ compounds that have commonly been identified in wood burning studies, and less common nitrogen-containing compounds. Specifically, from dung cookfires, we detected what we presume to be aromatic nitrogen-containing compounds with few or no oxygen atoms in them. Our inventory of chemical formulas is just the starting point for comprehensively characterizing particle-phase cookstove emissions. Future efforts should focus on the identification of compounds, precise emission factor quantification for specific compounds, evaluation of toxicity, and modeling the effect of these compounds on secondary air pollution formation in aging smoke plumes.

Acknowledgements

The authors would like to acknowledge Dr. Sneha Gautam's support of this project. He made sure the needs of the field technicians were met and acted as a consultant in the field. This research was supported by EPA STAR Grant R835425 Impacts of household sources on outdoor pollution at village and regional scales in India. The contents are solely the responsibility of the authors and do not necessarily represent the official views of the US EPA. US EPA does not endorse the purchase of any commercial products or services mentioned in the publication. The authors acknowledge NOAA grants NA16OAR4310101 (PNNL) and NA16OAR4310102 (UCI) for supporting nano-DESI and HPLC-PDA-HRMS analysis of samples. The HRMS measurements were performed at the W.R. Wiley Environmental Molecular Sciences Laboratory (EMSL) – a national scientific user facility located at PNNL, and sponsored by the Office of Biological and Environmental Research of the U.S. DOE. PNNL is operated for U.S. DOE by Battelle Memorial Institute under Contract No. DE-AC06-76RL0 1830.

References

Anastasio, C., Faust, B. C. and Rao, C. J.: Aromatic Carbonyl Compounds as Aqueous-Phase Photochemical Sources of Hydrogen Peroxide in Acidic Sulfate Aerosols, Fogs, and Clouds. 1. Non-Phenolic Methoxybenzaldehydes and Methoxyacetophenones with Reductants (Phenols), Environ. Sci. Technol., 31(1), 218–232, doi:10.1021/es960359g, 1997.

Araujo, J. A., Barajas, B., Kleinman, M., Wang, X., Bennett, B. J., Gong, K. W., Navab, M., Harkema, J., Sioutas, C., Lusis, A. J. and Nel, A. E.: Ambient Particulate Pollutants in the Ultrafine Range Promote Early Atherosclerosis and Systemic Oxidative Stress, Circ. Res., 102(5), 589–596, doi:10.1161/CIRCRESAHA.107.164970, 2008.

Balakrishnan, K., Sambandam, S., Ghosh, S., Mukhopadhyay, K., Vaswani, M., Arora, N. K., Jack, D., Pillariseti, A., Bates, M. N. and Smith, K. R.: Household Air Pollution Exposures of Pregnant Women Receiving Advanced Combustion Cookstoves in India: Implications for Intervention, Ann. Glob. Heal., 81(3), 375–385, doi:10.1016/j.aogh.2015.08.009, 2015.

Bluvshtein, N., Lin, P., Flores, J. M., Segev, L., Mazar, Y., Tas, E., Snider, G., Weagle, C., Brown, S. S., Laskin, A. and Rudich, Y.: Broadband optical properties of biomass-burning aerosol and identification of brown carbon chromophores, J. Geophys. Res. Atmos., 122(10), 5441–5456, doi:10.1002/2016JD026230, 2017.

Budisulistiorini, S. H., Riva, M., Williams, M., Chen, J., Itoh, M., Surratt, J. D. and Kuwata, M.: Light-Absorbing Brown Carbon Aerosol Constituents from Combustion of Indonesian Peat and Biomass, Environ. Sci. Technol., 51(8), 4415–4423, doi:10.1021/acs.est.7b00397, 2017.

Census of India: Households by Availability of Separate Kitchen and Type of Fuel Used for Cooking, [online] Available from: http://www.censusindia.gov.in/2011census/Hlo-series/HH10.html (Accessed 8 August 2017), 2011.

Chafe, Z. A., Brauer, M., Klimont, Z., Van Dingenen, R., Mehta, S., Rao, S., Riahi, K., Dentener, F. and Smith, K. R.: Household Cooking with Solid Fuels Contributes to Ambient PM2.5 Air Pollution and the Burden of Disease, Environ. Health Perspect., 122(12), 1314–1320, doi:10.1289/ehp.1206340, 2014.

Chen, Y. and Bond, T. C.: Light absorption by organic carbon from wood combustion, Atmos. Chem. Phys., 10(4), 1773–1787, doi:10.5194/acp-10-1773-2010, 2010.

Chen, Y., Roden, C. A. and Bond, T. C.: Characterizing Biofuel Combustion with Patterns of Real-Time Emission Data (PaRTED), Environ. Sci. Technol., 46(11), 6110–6117, doi:10.1021/es3003348, 2012.

Coggon, M. M., Veres, P. R., Yuan, B., Koss, A., Warneke, C., Gilman, J. B., Lerner, B. M., Peischl, J., Aikin, K. C., Stockwell, C. E., Hatch, L. E., Ryerson, T. B., Roberts, J. M., Yokelson, R. J. and de Gouw, J. A.: Emissions of nitrogen-containing organic compounds from the burning of herbaceous and arboraceous biomass: Fuel composition dependence and the variability of commonly used nitrile tracers, Geophys. Res. Lett., 43(18), 9903–9912, doi:10.1002/2016GL070562, 2016.

Collard, F.-X. and Blin, J.: A review on pyrolysis of biomass constituents: Mechanisms and composition of the products obtained from the conversion of cellulose, hemicelluloses and lignin, Renew. Sustain. Energy Rev., 38, 594–608, doi:10.1016/j.rser.2014.06.013, 2014.

Crutzen, P. J. and Andreae, M. O.: Biomass Burning in the Tropics - Impact on Atmospheric Chemistry and Biogeochemical Cycles, Science, 250(4988), 1669–1678, doi:10.1126/science.250.4988.1669, 1990.

Feng, Y., Ramanathan, V. and Kotamarthi, V. R.: Brown carbon: a significant atmospheric absorber of solar radiation?,

Atmos. Chem. Phys., 13(17), 8607–8621, doi:10.5194/acp-13-8607-2013, 2013.

Finlayson-Pitts, B. J. and Pitts, J. N.: Chemistry of the Upper and Lower Atmosphere: Theory, Experiments, and Applications, Academic Press, San Diego, CA., 2000.

Gautam, S., Edwards, R., Yadav, A., Weltman, R., Pillarsetti, A., Arora, N. K. and Smith, K. R.: Probe-based measurements of moisture in dung fuel for emissions measurements, Energy Sustain. Dev., 35, 1–6, doi:10.1016/j.esd.2016.09.003, 2016.

Global Alliance for Clean Cookstoves: Protocols: Water Boiling Test, [online] Available from: http://cleancookstoves.org/technology-and-fuels/testing/protocols.html, 2014.

Guttikunda, S., Jawahar, P., Gota, S. and KA, N.: UrbanEmissions.info, [online] Available from: http://www.urbanemissions.info/ (Accessed 10 August 2017), 2016.

Hatch, L. E., Luo, W., Pankow, J. F., Yokelson, R. J., Stockwell, C. E. and Barsanti, K. C.: Identification and quantification of gaseous organic compounds emitted from biomass burning using two-dimensional gas chromatography–time-of-flight mass spectrometry, Atmos. Chem. Phys., 15(4), 1865–1899, doi:10.5194/acp-15-1865-2015, 2015.

Hosseini, S., Urbanski, S. P., Dixit, P., Qi, L., Burling, I. R., Yokelson, R. J., Johnson, T. J., Shrivastava, M., Jung, H. S., Weise, D. R., Miller, J. W. and Cocker, D. R.: Laboratory characterization of PM emissions from combustion of wildland biomass fuels, J. Geophys. Res., 118(17), 9914–9929, doi:10.1002/jgrd.50481, 2013.

Hughey, C. A., Hendrickson, C. L., Rodgers, R. P., Marshall, A. G. and Qian, K.: Kendrick Mass Defect Spectrum: A Compact Visual Analysis for Ultrahigh-Resolution Broadband Mass Spectra, Anal. Chem., 73(19), 4676–4681, doi:10.1021/AC010560W, 2001.

Jayarathne, T., Stockwell, C. E., Bhave, P. V., Praveen, P. S., Rathnayake, C. M., Islam, M. R., Panday, A. K., Adhikari, S., Maharjan, R., Goetz, J. D., DeCarlo, P. F., Saikawa, E., Yokelson, R. J. and Stone, E. A.: Nepal Ambient Monitoring and Source Testing Experiment (NAMaSTE): Emissions of particulate matter from wood and dung cooking fires, garbage and crop residue burning, brick kilns, and other sources, Atmos. Chem. Phys. Discuss., 1–51, doi:10.5194/acp-2017-510, 2017.

Johnson, M., Edwards, R., Alatorre Frenk, C. and Masera, O.: In-field greenhouse gas emissions from cookstoves in rural Mexican households, Atmos. Environ., 42(6), 1206–1222, doi:10.1016/j.atmosenv.2007.10.034, 2008.

Johnson, M., Edwards, R., Ghilardi, A., Berrueta, V., Gillen, D., Frenk, C. A. and Masera, O.: Quantification of Carbon Savings from Improved Biomass Cookstove Projects, Environ. Sci. Technol., 43(7), 2456–2462, doi:10.1021/es801564u, 2009.

Kirchstetter, T. W., Novakov, T. and Hobbs, P. V.: Evidence that the spectral dependence of light absorption by aerosols is affected by organic carbon, J. Geophys. Res. Atmos., 109(D21), doi:10.1029/2004JD004999, 2004.

Kituyi, E., Marufu, L., Wandiga, S. O., Jumba, I. O., Andreae, M. O. and Helas, G.: Carbon monoxide and nitric oxide from biofuel fires in Kenya, Energy Convers. Manag., 42(13), 1517–1542, doi:10.1016/S0196-8904(00)00158-8, 2001.

Lack, D. A. and Langridge, J. M.: On the attribution of black and brown carbon light absorption using the Ångström exponent, Atmos. Chem. Phys., 13(20), 10535–10543, doi:10.5194/acp-13-10535-2013, 2013.

Laskin, A., Smith, J. S. and Laskin, J.: Molecular Characterization of Nitrogen-Containing Organic Compounds in Biomass

Burning Aerosols Using High-Resolution Mass Spectrometry, Environ. Sci. Technol., 43(10), 3764–3771, doi:10.1021/es803456n, 2009.

Laskin, A., Laskin, J. and Nizkorodov, S. A.: Chemistry of Atmospheric Brown Carbon, Chem. Rev., 115(10), 4335–4382, doi:10.1021/cr5006167, 2015.

5 Laskin, J., Laskin, A., Roach, P. J., Slysz, G. W., Anderson, G. A., Nizkorodov, S. A., Bones, D. L. and Nguyen, L. Q.: High-Resolution Desorption Electrospray Ionization Mass Spectrometry for Chemical Characterization of Organic Aerosols, Anal. Chem., 82(5), 2048–2058, doi:10.1021/ac902801f, 2010.

Lee, S., Baumann, K., Schauer, J. J., Sheesley, R. J., Naeher, L. P., Meinardi, S., Blake, D. R., Edgerton, E. S., Russell, A. G. and Clements, M.: Gaseous and particulate emissions from prescribed burning in Georgia, Environ. Sci. Technol., 39(23),
10 9049–9056, doi:10.1021/es051583l, 2005.

Lelieveld, J., Evans, J. S., Fnais, M., Giannadaki, D. and Pozzer, A.: The contribution of outdoor air pollution sources to premature mortality on a global scale, Nature, 525(7569), 367–371, doi:10.1038/nature15371, 2015.

Lin, P., Rincon, A. G., Kalberer, M. and Yu, J. Z.: Elemental Composition of HULIS in the Pearl River Delta Region, China: Results Inferred from Positive and Negative Electrospray High Resolution Mass Spectrometric Data, Environ. Sci. Technol.,
15 46(14), 7454–7462, doi:10.1021/es300285d, 2012.

Lin, P., Laskin, J., Nizkorodov, S. A. and Laskin, A.: Revealing Brown Carbon Chromophores Produced in Reactions of Methylglyoxal with Ammonium Sulfate, Environ. Sci. Technol., 49(24), 14257–14266, doi:10.1021/acs.est.5b03608, 2015.

Lin, P., Aiona, P. K., Li, Y., Shiraiwa, M., Laskin, J., Nizkorodov, S. A. and Laskin, A.: Molecular Characterization of Brown Carbon in Biomass Burning Aerosol Particles, Environ. Sci. Technol., 50(21), 11815–11824,
20 doi:10.1021/acs.est.6b03024, 2016.

Lin, P., Bluvshtein, N., Rudich, Y., Nizkorodov, S., Laskin, J. and Laskin, A.: Molecular Chemistry of Atmospheric Brown Carbon Inferred from a Nationwide Biomass-Burning Event, Environ. Sci. Technol., 51(20), 11561–11570, doi:10.1021/acs.est.7b02276, 2017.

Lobert, J. M., Keene, W. C., Logan, J. A. and Yevich, R.: Global chlorine emissions from biomass burning: Reactive
25 Chlorine Emissions Inventory, J. Geophys. Res. Atmos., 104(D7), 8373–8389, doi:10.1029/1998JD100077, 1999.

Ludwig, J., Marufu, L. T., Huber, B., Andreae, M. O. and Helas, G.: Domestic Combustion of Biomass Fuels in Developing Countries: A Major Source of Atmospheric Pollutants, J. Atmos. Chem., 44(1), 23–37, doi:10.1023/A:1022159910667, 2003.

Mukhopadhyay, R., Sambandam, S., Pillarisetti, A., Jack, D., Mukhopadhyay, K., Balakrishnan, K., Vaswani, M., Bates, M.
30 N., Kinney, P. L., Arora, N. and Smith, K. R.: Cooking practices, air quality, and the acceptability of advanced cookstoves in Haryana, India: an exploratory study to inform large-scale interventions., Glob. Health Action, 5, 1–13, doi:10.3402/gha.v5i0.19016, 2012.

Pandey, A., Pervez, S. and Chakrabarty, R. K.: Filter-based measurements of UV–vis mass absorption cross sections of organic carbon aerosol from residential biomass combustion: Preliminary findings and sources of uncertainty, J. Quant.

Spectrosc. Radiat. Transf., 182, 296–304, doi:10.1016/j.jqsrt.2016.06.023, 2016.

Pillarisetti, A., Vaswani, M., Jack, D., Balakrishnan, K., Bates, M. N., Arora, N. K. and Smith, K. R.: Patterns of Stove Usage after Introduction of an Advanced Cookstove: The Long-Term Application of Household Sensors, Environ. Sci. Technol., 48(24), 14525–14533, doi:10.1021/es504624c, 2014.

5   Pluskal, T., Castillo, S., Villar-Briones, A. and Orešič, M.: MZmine 2: Modular framework for processing, visualizing, and analyzing mass spectrometry-based molecular profile data, BMC Bioinformatics, 11(1), 395, doi:10.1186/1471-2105-11-395, 2010.

Purcell, J. M., Rodgers, R. P., Hendrickson, C. L. and Marshall, A. G.: Speciation of nitrogen containing aromatics by atmospheric pressure photoionization or electrospray ionization fourier transform ion cyclotron resonance mass

10   spectrometry, J. Am. Soc. Mass Spectrom., 18(7), 1265–1273, doi:10.1016/j.jasms.2007.03.030, 2007.

Roach, P. J., Laskin, J. and Laskin, A.: Molecular Characterization of Organic Aerosols Using Nanospray-Desorption/Electrospray Ionization-Mass Spectrometry, Anal. Chem., 82(19), 7979–7986, doi:10.1021/ac101449p, 2010a.

Roach, P. J., Laskin, J. and Laskin, A.: Nanospray desorption electrospray ionization: an ambient method for liquid-extraction surface sampling in mass spectrometry, Analyst, 135(9), 2233–2236, doi:10.1039/c0an00312c, 2010b.

15   Roach, P. J., Laskin, J. and Laskin, A.: Higher-Order Mass Defect Analysis for Mass Spectra of Complex Organic Mixtures, Anal. Chem., 83(12), 4924–4929, doi:10.1021/ac200654j, 2011.

Roden, C. A., Bond, T. C., Conway, S., Osorto Pinel, A. B., MacCarty, N. and Still, D.: Laboratory and field investigations of particulate and carbon monoxide emissions from traditional and improved cookstoves, Atmos. Environ., 43(6), 1170–1181, doi:10.1016/j.atmosenv.2008.05.041, 2009.

20   Saleh, R., Robinson, E. S., Tkacik, D. S., Ahern, A. T., Liu, S., Aiken, A. C., Sullivan, R. C., Presto, A. A., Dubey, M. K., Yokelson, R. J., Donahue, N. M. and Robinson, A. L.: Brownness of organics in aerosols from biomass burning linked to their black carbon content, Nat. Geosci., 7, 647–650, 2014.

Simoneit, B. R. T.: Biomass burning — a review of organic tracers for smoke from incomplete combustion, Appl. Geochemistry, 17(3), 129–162, doi:10.1016/S0883-2927(01)00061-0, 2002.

25   Simoneit, B. R. T., Rogge, W. F., Mazurek, M. A., Standley, L. J., Hildemann, L. M. and Cass, G. R.: Lignin pyrolysis products, lignans, and resin acids as specific tracers of plant classes in emissions from biomass combustion, Environ. Sci. Technol., 27(12), 2533–2541, doi:10.1021/es00048a034, 1993.

Simoneit, B. R. T., Schauer, J. J., Nolte, C. G., Oros, D. R., Elias, V. O., Fraser, M. P., Rogge, W. F. and Cass, G. R.: Levoglucosan, a tracer for cellulose in biomass burning and atmospheric particles, Atmos. Environ., 33(2), 173–182,

30   doi:10.1016/S1352-2310(98)00145-9, 1999.

Smith, J. S., Laskin, A. and Laskin, J.: Molecular Characterization of Biomass Burning Aerosols Using High-Resolution Mass Spectrometry, Anal. Chem., 81(4), 1512–1521, doi:10.1021/ac8020664, 2009.

Smith, K. R., Bruce, N., Balakrishnan, K., Adair-Rohani, H., Balmes, J., Chafe, Z., Dherani, M., Hosgood, H. D., Mehta, S., Pope, D., Rehfuess, E. and HAP CRA Risk Expert Group: Millions dead: how do we know and what does it mean? Methods

used in the comparative risk assessment of household air pollution., Annu. Rev. Public Health, 35, 185–206, doi:10.1146/annurev-publhealth-032013-182356, 2014.

Stockwell, C. E., Christian, T. J., Goetz, J. D., Jayarathne, T., Bhave, P. V., Praveen, P. S., Adhikari, S., Maharjan, R., DeCarlo, P. F., Stone, E. A., Saikawa, E., Blake, D. R., Simpson, I. J., Yokelson, R. J. and Panday, A. K.: Nepal Ambient Monitoring and Source Testing Experiment (NAMaSTE): emissions of trace gases and light-absorbing carbon from wood and dung cooking fires, garbage and crop residue burning, brick kilns, and other sources, Atmos. Chem. Phys., 16(17), 11043–11081, doi:10.5194/acp-16-11043-2016, 2016.

Sullivan, A. P., May, A. A., Lee, T., McMeeking, G. R., Kreidenweis, S. M., Akagi, S. K., Yokelson, R. J., Urbanski, S. P. and Collett Jr., J. L.: Airborne characterization of smoke marker ratios from prescribed burning, Atmos. Chem. Phys., 14(19), 10535–10545, doi:10.5194/acp-14-10535-2014, 2014.

Talrose, V., Yermakov, A. N., Usov, A. A., Goncharova, A. A., Leskin, A. N., Messineva, N. A., Trusova, N. V. and Efimkina, M. V.: UV/Visible Spectra, in NIST Chemistry WebBook, NIST Standard Reference Database Number 69, edited by P. J. Linstrom and W. G. Mallard, National Institute of Standards and Technology, Gaithersburg MD, 20899., 2017.

Wan, E. C. H. and Yu, J. Z.: Determination of sugar compounds in atmospheric aerosols by liquid chromatography combined with positive electrospray ionization mass spectrometry, J. Chromatogr. A, 1107(1–2), 175–181, doi:10.1016/j.chroma.2005.12.062, 2006.

Wang, Y., Hu, M., Lin, P., Guo, Q., Wu, Z., Li, M., Zeng, L., Song, Y., Zeng, L., Wu, Y., Guo, S., Huang, X. and He, L.: Molecular Characterization of Nitrogen-Containing Organic Compounds in Humic-like Substances Emitted from Straw Residue Burning, Environ. Sci. Technol., 51(11), 5951–5961, doi:10.1021/acs.est.7b00248, 2017.

Willoughby, A., Wozniak, A. and Hatcher, P.: Detailed Source-Specific Molecular Composition of Ambient Aerosol Organic Matter Using Ultrahigh Resolution Mass Spectrometry and ^{1}H NMR, Atmosphere, 7(6), 79, doi:10.3390/atmos7060079, 2016.

Xiao, Q. Y., Saikawa, E., Yokelson, R. J., Chen, P. F., Li, C. L. and Kang, S. C.: Indoor air pollution from burning yak dung as a household fuel in Tibet, Atmos. Environ., 102, 406–412, doi:10.1016/j.atmosenv.2014.11.060, 2015.

Figure 1: The field site and set-up for cooking events. A) The kitchen set-up at the field site. B) The stoves and fuels used in this study: *angithi***, dung-burning** *chulha***, and brushwood-burning** *chulha***.**
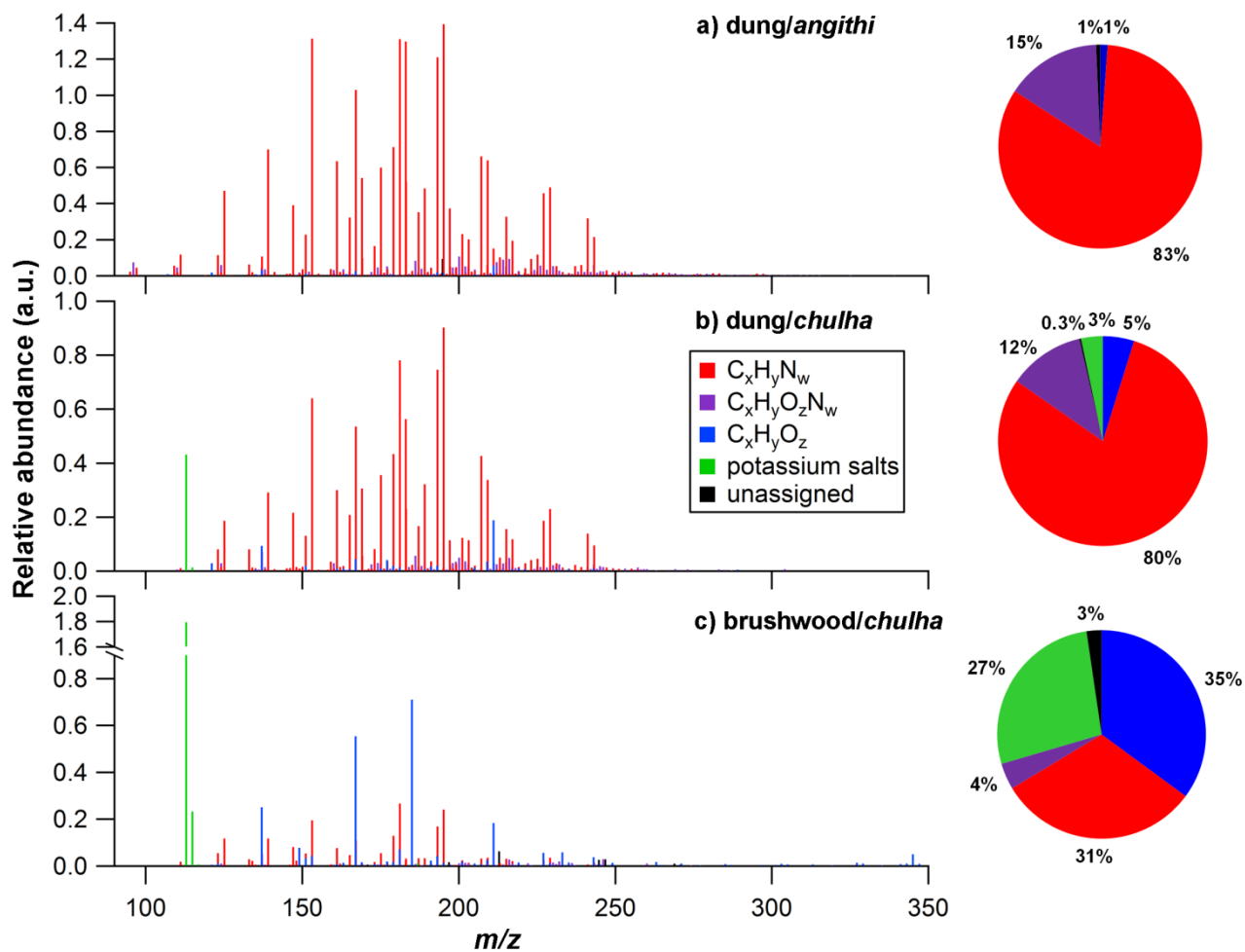
Figure 2: Representative nano-DESI mass spectra collected for a) dung/*angithi* b) dung/*chulha* and c) brushwood/*chulha* cookfires. Relative abundance is plotted against *m/z*. Peaks are colored by their elemental makeup, $C_xH_yN_w$ (red), $C_xH_yO_zN_w$ (purple), $C_xH_yO_z$ (blue), potassium salts (green), and unassigned (black). The pie charts illustrate the fraction of count-based, normalized peak abundance that is attributed to each elemental category.
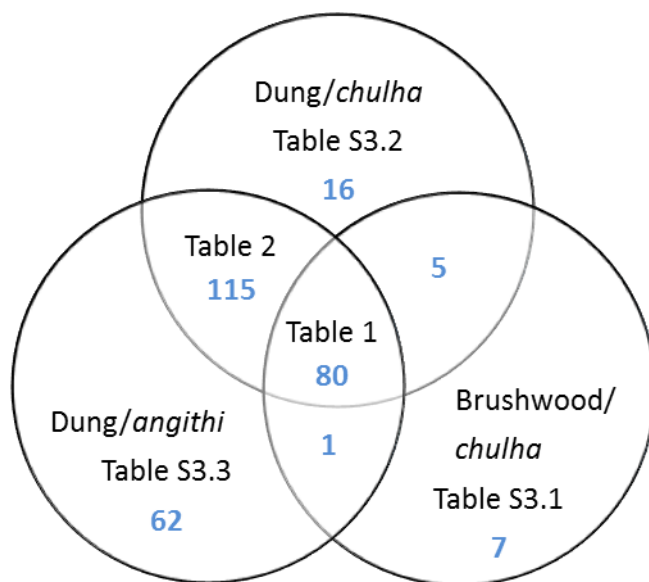
Figure 3: An overview of the particle-phase compounds inventory based on the results of molecular characterization using nano-DESI-HRMS. Each area of the Venn diagram contains the bolded number of reproducibly-detected formulas in blue as well as the Table that lists peaks for each category. Merging all the tables listed here provides a complete inventory of compounds detected in this study.
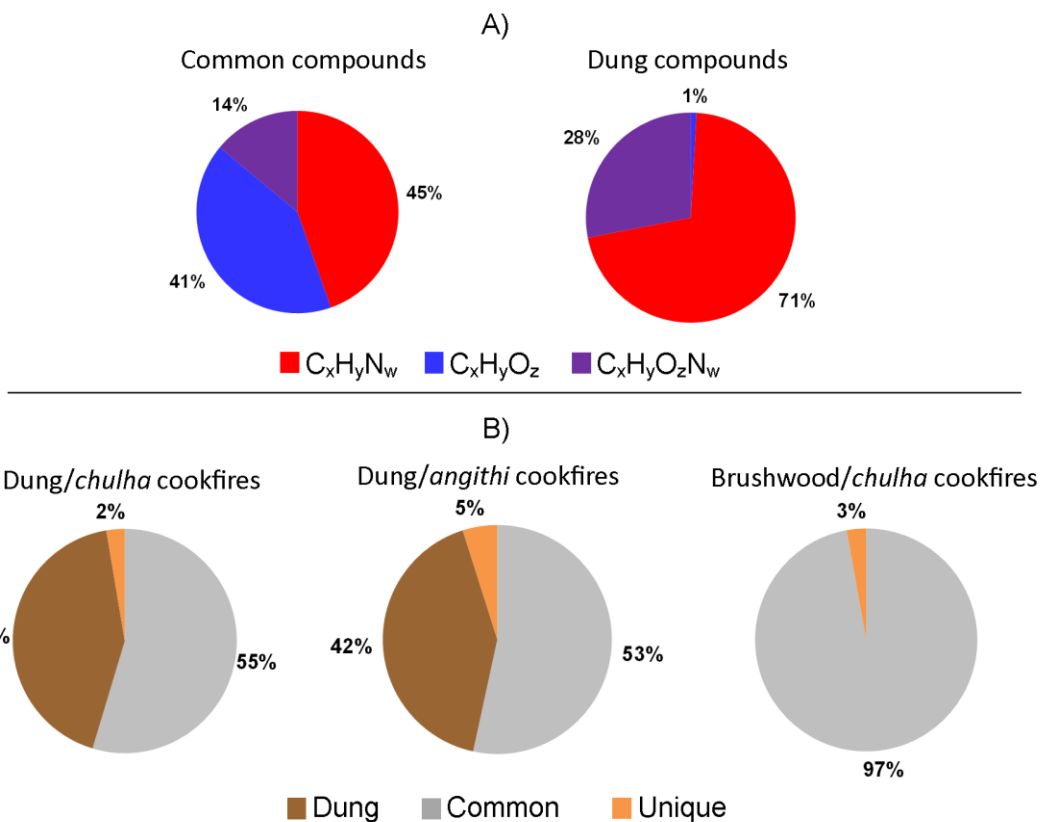
Figure 4: A summary of the inventory in terms of the count-based, normalized peak abundances. A) Contribution of PM$_{2.5}$ compounds to each elemental formula category for those found in all cookfires and those found in all dung-burning cookfires. B) The compounds by cookstove type classified as compounds common to all cookfires in grey, compounds common to all dung cookfires in brown, and unique compounds in orange.
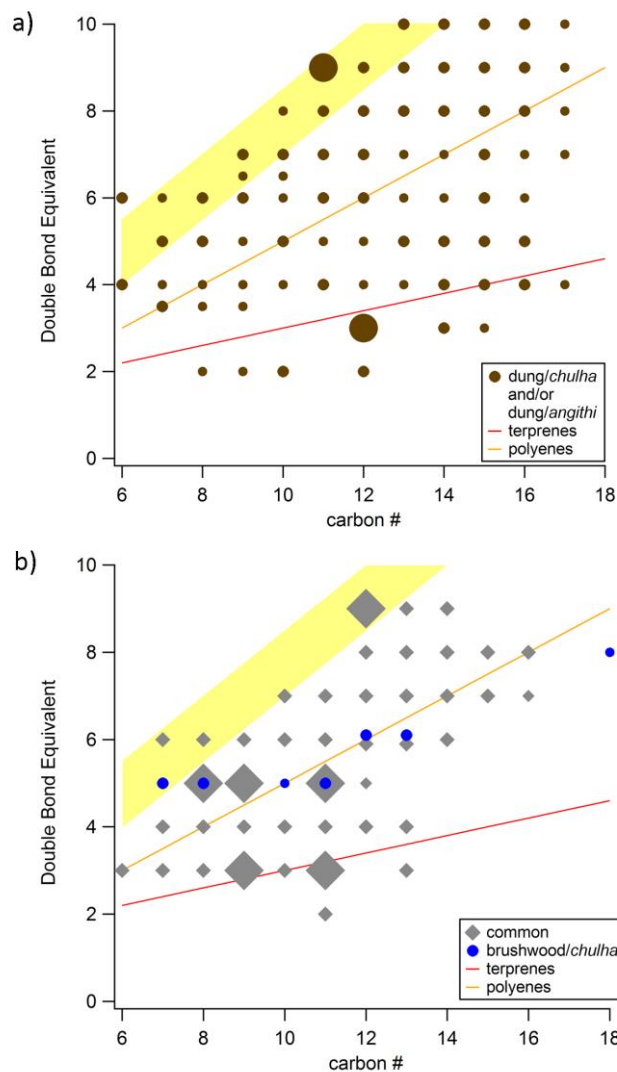
Figure 5: Double bond equivalent (DBE) as a function of the carbon number for a) a combined set of compounds detected from all dung cookfires (brown circle) and b) compounds all cookfires have in common (grey diamond) as well as compounds exclusively found in brushwood (blue circle). Markers representing one or multiple species are sized by their LOW, MEDIUM, and HIGH designations. The curves illustrate theoretically where terpenes (red) and polyenes (green) would fall. Similarly, the yellow-shaded region shows where PAHs would appear, including: cata-condensed PAHs with 0, 1, and 2 heterocyclic nitrogen atoms and circular PAHs.

Acridine
$C_{13}H_9N$

Phenoxazine
$C_{12}H_9ON$

β-Carboline
$C_{11}H_8N_2$
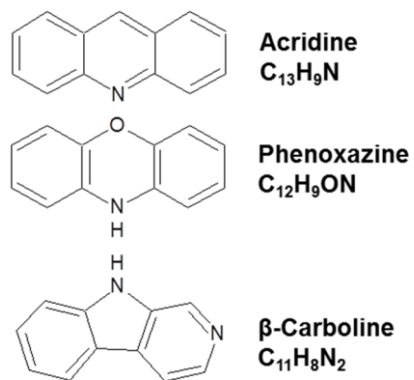
Figure 6: Possible structures of N-heterocyclic PAHs found in dung cookfire emissions. $C_{13}H_9N$ was detected reproducibly in dung/*chulha* emissions only, while $C_{12}H_9ON$ and $C_{11}H_8N_2$ were reproducibly detected in all dung cookfires.
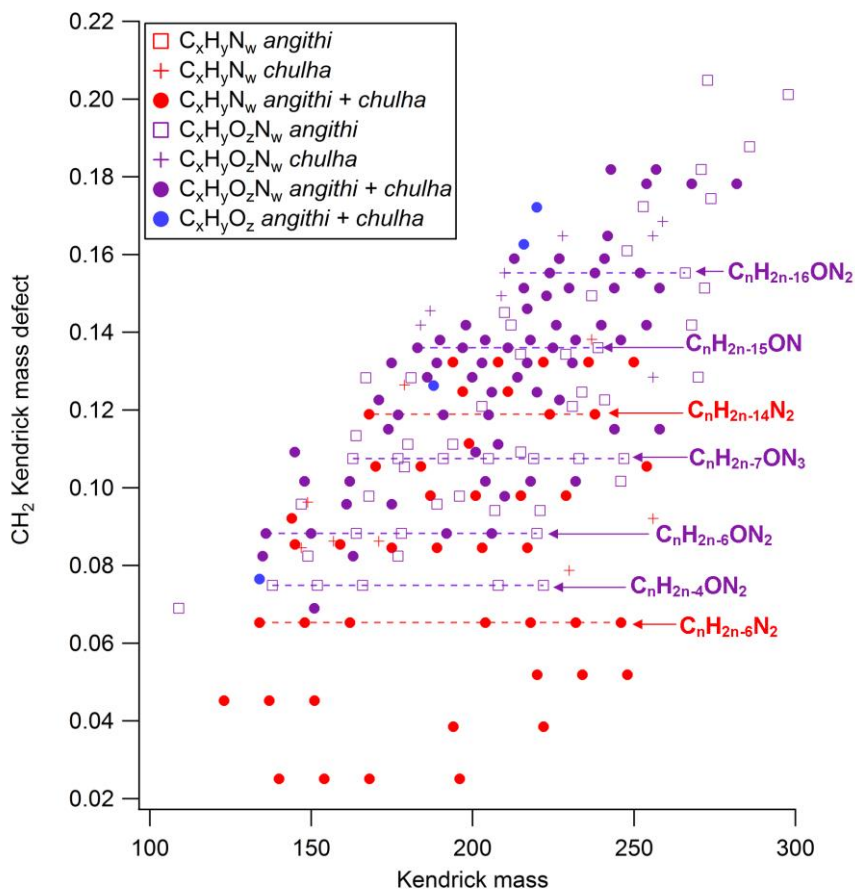
Figure 7: The CH$_2$ Kendrick mass defect plot for compounds emitted only from dung stoves. The marker color determines the compound category for C$_x$H$_y$N$_w$ compounds (red), C$_x$H$_y$O$_z$ (blue), or C$_x$H$_y$O$_z$N$_w$ (purple). Marker shape indicates the stove(s) that reproducibly produced the compound: *chulha* and *angithi* (●), *angithi* (□), or *chulha* (+). Homologous series are identified with dotted horizontal lines suggesting they have similar structures.
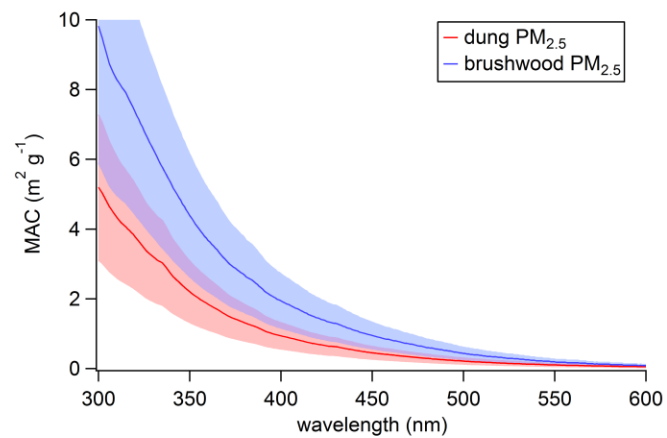
Figure 8: Comparing MAC$_{bulk}$ (m^2 g^{-1}) for organic solvent extractable material from brushwood/*chulha* (blue) and dung/*chulha* (red) samples. Shaded regions represent errors due to extraction efficiency and sampling flow rates.
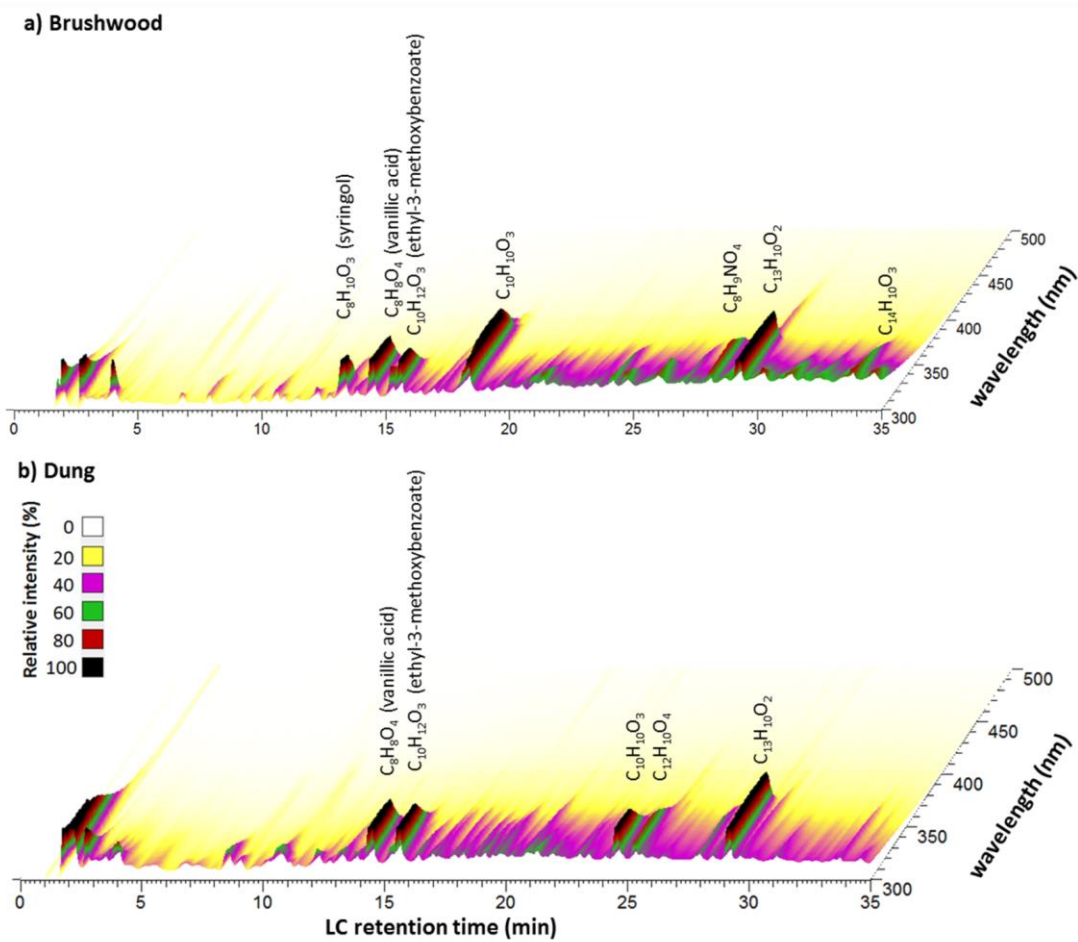
Figure 9: HPLC-PDA chromatogram showing BrC chromophores detected in the emmision samples from a) brushwood and b) dung cookfires. Highly-absorbing molecules and their corresponding PDA retention times are given above the peak.
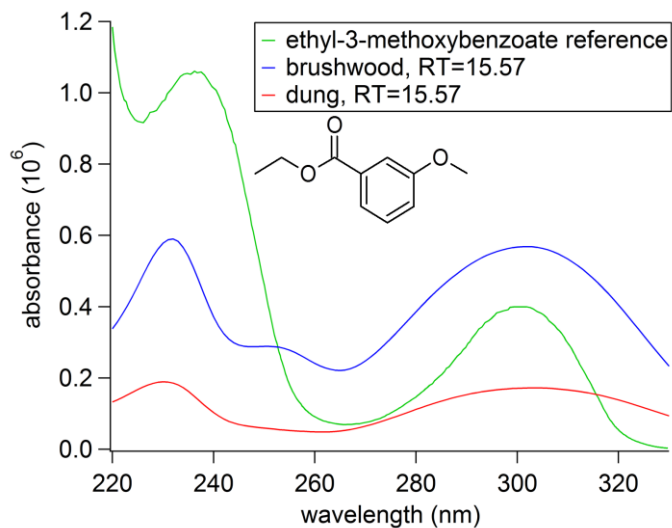
Figure 10: UV-Vis absorption spectra from the PDA analysis of cookstove BBOA samples. The blue and red curves represent the background-subtracted absorbance at retention time of 15.57 min for brushwood-derived PM$_{2.5}$ and dung-derived PM$_{2.5}$, respectively. The reference absorption spectrum of ethyl-3-methoxybenzoate (green) was reproduced from the NIST Chemistry WebBook database (Talrose et al., 2017). The structure of ethyl-3-methoxybenzoate is pictured.

Table 1: List of common compounds found in all PM$_{2.5}$ samples regardless of fuel or stove type. Tentative molecular structure assignments are listed when the compound has previously been identified in the chemical biomass-burning literature, supported by the references in the last column. Count-based, normalized peak abundances are designated LOW (<1%), MEDIUM (1-9.99%), HIGH (10-100%). All species were detected as protonated ions.

Observed m/z	Calculated m/z	Chemical formula of neutral species	DBE	Relative average abundance	Tentative assignment(s)	References
111.091	111.092	$C_6H_{10}N_2$	3	MEDIUM		(Smith et al., 2009)
121.064	121.065	C_8H_8O	5	MEDIUM		
123.091	123.092	$C_7H_{10}N_2$	4	MEDIUM		
124.075	124.076	C_7H_9ON	4	MEDIUM		
125.107	125.107	$C_7H_{12}N_2$	3	MEDIUM		(Smith et al., 2009)
133.075	133.076	$C_8H_8N_2$	6	MEDIUM		(Laskin et al., 2009)
134.071	134.071	$C_7H_7N_3$	6	MEDIUM		(Laskin et al., 2009)
137.059	137.060	$C_8H_8O_2$	5	HIGH	Anisaldehyde	(Simoneit et al., 1993; Smith et al., 2009)
137.106	137.107	$C_8H_{12}N_2$	4	MEDIUM		(Smith et al., 2009)
138.090	138.091	$C_8H_{11}ON$	4	LOW		
139.122	139.123	$C_8H_{14}N_2$	3	MEDIUM		(Smith et al., 2009)
147.091	147.092	$C_9H_{10}N_2$	6	MEDIUM		
151.074	151.075	$C_9H_{10}O_2$	5	MEDIUM	Vinylguaiacol	
151.122	151.123	$C_9H_{14}N_2$	4	MEDIUM		
153.138	153.139	$C_9H_{16}N_2$	3	HIGH		
159.091	159.092	$C_{10}H_{10}N_2$	7	MEDIUM		(Laskin et al., 2009)
160.075	160.076	$C_{10}H_9ON$	7	MEDIUM		(Laskin et al., 2009)
161.059	161.060	$C_{10}H_8O_2$	7	MEDIUM		
161.106	161.107	$C_{10}H_{12}N_2$	6	MEDIUM		
162.102	162.103	$C_9H_{11}N_3$	6	LOW		
163.074	163.075	$C_{10}H_{10}O_2$	6	MEDIUM		
165.138	165.139	$C_{10}H_{16}N_2$	4	MEDIUM		
167.069	167.070	$C_9H_{10}O_3$	5	HIGH	Veratraldehyde	(Simoneit et al., 1993)
167.153	167.154	$C_{10}H_{18}N_2$	3	MEDIUM		
173.106	173.107	$C_{11}H_{12}N_2$	7	MEDIUM		
174.090	174.091	$C_{11}H_{11}ON$	7	MEDIUM		
175.074	175.075	$C_{11}H_{10}O_2$	7	MEDIUM		
175.122	175.123	$C_{11}H_{14}N_2$	6	MEDIUM		
177.053	177.055	$C_{10}H_8O_3$	7	MEDIUM		

177.090	177.091	$C_{11}H_{12}O_2$	6	MEDIUM		
177.101	177.102	$C_{10}H_{12}ON_2$	6	LOW		
177.137	177.139	$C_{11}H_{16}N_2$	5	LOW		(Laskin et al., 2009)
179.069	179.070	$C_{10}H_{10}O_3$	6	MEDIUM	Coniferaldehyde	
179.153	179.154	$C_{11}H_{18}N_2$	4	MEDIUM		
181.169	181.170	$C_{11}H_{20}N_2$	3	HIGH		
183.090	183.092	$C_{12}H_{10}N_2$	9	HIGH		
183.184	183.186	$C_{11}H_{22}N_2$	2	MEDIUM		
186.090	186.091	$C_{12}H_{11}ON$	8	MEDIUM		(Laskin et al., 2009)
187.122	187.123	$C_{12}H_{14}N_2$	7	MEDIUM		
188.106	188.107	$C_{12}H_{13}ON$	7	MEDIUM		
189.101	189.102	$C_{11}H_{12}ON_2$	7	MEDIUM		(Laskin et al., 2009)
189.137	189.139	$C_{12}H_{16}N_2$	6	MEDIUM		
191.069	191.070	$C_{11}H_{10}O_3$	7	MEDIUM		
191.117	191.118	$C_{11}H_{14}ON_2$	6	LOW		
191.153	191.154	$C_{12}H_{18}N_2$	5	LOW		
193.085	193.086	$C_{11}H_{12}O_3$	6	MEDIUM		
193.169	193.170	$C_{12}H_{20}N_2$	4	MEDIUM		
197.106	197.107	$C_{13}H_{12}N_2$	9	MEDIUM		
199.122	199.123	$C_{13}H_{14}N_2$	8	LOW		
200.106	200.107	$C_{13}H_{13}ON$	8	MEDIUM		
201.137	201.139	$C_{13}H_{16}N_2$	7	MEDIUM		
202.085	202.086	$C_{12}H_{11}O_2N$	8	MEDIUM		(Laskin et al., 2009)
203.117	203.118	$C_{12}H_{14}ON_2$	7	MEDIUM		
203.153	203.154	$C_{13}H_{18}N_2$	6	MEDIUM		
205.085	205.086	$C_{12}H_{12}O_3$	7	MEDIUM		
207.184	207.186	$C_{13}H_{22}N_2$	4	MEDIUM		
209.079	209.081	$C_{11}H_{12}O_4$	6	MEDIUM		
209.200	209.201	$C_{13}H_{24}N_2$	3	MEDIUM		
211.095	211.096	$C_{11}H_{14}O_4$	5	HIGH	Syringylethanone/ trimethoxyphenylethanone	(Simoneit et al., 1993)
211.121	211.123	$C_{14}H_{14}N_2$	9	MEDIUM		
213.137	213.139	$C_{14}H_{16}N_2$	8	MEDIUM		(Laskin et al., 2009)
214.121	214.123	$C_{14}H_{15}ON$	8	MEDIUM		
215.153	215.154	$C_{14}H_{18}N_2$	7	MEDIUM		
216.100	216.102	$C_{13}H_{13}O_2N$	8	MEDIUM		
217.132	217.134	$C_{13}H_{16}ON_2$	7	MEDIUM		

Observed m/z	Calculated m/z	Chemical formula of neutral species	DBE	Relative average abundance
217.168	217.170	$C_{14}H_{20}N_2$	6	MEDIUM
219.100	219.102	$C_{13}H_{14}O_3$	7	MEDIUM
227.153	227.154	$C_{15}H_{18}N_2$	8	MEDIUM
229.132	229.134	$C_{14}H_{16}ON_2$	8	MEDIUM
229.168	229.170	$C_{15}H_{20}N_2$	7	MEDIUM
230.116	230.118	$C_{14}H_{15}O_2N$	8	MEDIUM
231.147	231.149	$C_{14}H_{18}ON_2$	7	LOW
232.095	232.097	$C_{13}H_{13}O_3N$	8	MEDIUM
235.095	235.096	$C_{13}H_{14}O_4$	7	MEDIUM
241.168	241.170	$C_{16}H_{20}N_2$	8	MEDIUM
243.147	243.149	$C_{15}H_{18}ON_2$	8	MEDIUM
243.184	243.186	$C_{16}H_{22}N_2$	7	LOW
244.131	244.133	$C_{15}H_{17}O_2N$	8	MEDIUM
246.111	246.112	$C_{14}H_{15}O_3N$	8	MEDIUM
249.110	249.112	$C_{14}H_{16}O_4$	7	MEDIUM

Table 2: List of compounds found exclusively in the emissions from dung cookfires, regardless of stove type. The labels for the peak abundances are the same as in Table 1. All species were detected as protonated ions unless otherwise noted.

Observed m/z	Calculated m/z	Chemical formula of neutral species	DBE	Relative average abundance
124.099	124.099	$C_7H_{12}N_2$*	3	MEDIUM
135.080	135.080	$C_9H_{10}O$	5	LOW
135.092	135.092	$C_8H_{10}N_2$	5	MEDIUM
136.076	136.076	C_8H_9ON	5	LOW
137.071	137.071	$C_7H_8ON_2$	5	MEDIUM
138.115	138.115	$C_8H_{14}N_2$*	3	LOW
141.138	141.139	$C_8H_{16}N_2$	2	LOW
145.076	145.076	$C_9H_8N_2$	7	MEDIUM
146.060	146.060	C_9H_7ON	7	MEDIUM
146.084	146.084	$C_9H_{10}N_2$*	6	LOW
149.071	149.071	$C_8H_8ON_2$	6	LOW
149.107	149.107	$C_9H_{12}N_2$	5	LOW
151.086	151.087	$C_8H_{10}ON_2$	5	LOW
152.107	152.107	$C_9H_{13}ON$	4	LOW
152.130	152.131	$C_9H_{16}N_2$*	3	LOW

155.154	155.154	$C_9H_{18}N_2$	2	LOW
160.099	160.099	$C_{10}H_{12}N_2^*$	6	LOW
162.091	162.091	$C_{10}H_{11}ON$	6	LOW
163.086	163.087	$C_9H_{10}ON_2$	6	MEDIUM
163.123	163.123	$C_{10}H_{14}N_2$	5	MEDIUM
164.107	164.107	$C_{10}H_{13}ON$	5	LOW
169.076	169.076	$C_{11}H_8N_2$	9	HIGH
169.170	169.170	$C_{10}H_{20}N_2$	2	MEDIUM
171.091	171.092	$C_{11}H_{10}N_2$	8	MEDIUM
172.075	172.076	$C_{11}H_9ON$	8	MEDIUM
175.086	175.087	$C_{10}H_{10}ON_2$	7	MEDIUM
176.070	176.071	$C_{10}H_9O_2N$	7	LOW
176.107	176.107	$C_{11}H_{13}ON$	6	LOW
176.118	176.118	$C_{10}H_{13}N_3$	6	LOW
178.086	178.086	$C_{10}H_{11}O_2N$	6	LOW
184.075	184.076	$C_{12}H_9ON$	9	MEDIUM
185.107	185.107	$C_{12}H_{12}N_2$	8	MEDIUM
187.086	187.087	$C_{11}H_{10}ON_2$	8	MEDIUM
188.118	188.118	$C_{11}H_{13}N_3$	7	LOW
189.091	189.091	$C_{12}H_{12}O_2$	7	LOW
190.086	190.086	$C_{11}H_{11}O_2N$	7	MEDIUM
190.133	190.134	$C_{11}H_{15}N_3$	6	MEDIUM
191.081	191.082	$C_{10}H_{10}O_2N_2$	7	LOW
192.102	192.102	$C_{11}H_{13}O_2N$	6	LOW
193.133	193.134	$C_{11}H_{16}ON_2$	5	LOW
195.091	195.092	$C_{13}H_{10}N_2$	10	MEDIUM
195.185	195.186	$C_{12}H_{22}N_2$	3	HIGH
197.201	197.201	$C_{12}H_{24}N_2$	2	MEDIUM
198.091	198.091	$C_{13}H_{11}ON$	9	MEDIUM
198.102	198.103	$C_{12}H_{11}N_3$	9	LOW
199.086	199.087	$C_{12}H_{10}ON_2$	9	MEDIUM
200.118	200.118	$C_{12}H_{13}N_3$	8	LOW
201.102	201.102	$C_{12}H_{12}ON_2$	8	MEDIUM
202.122	202.123	$C_{13}H_{15}ON$	7	LOW
202.133	202.134	$C_{12}H_{15}N_3$	7	LOW
204.101	204.102	$C_{12}H_{13}O_2N$	7	LOW
204.149	204.150	$C_{12}H_{17}N_3$	6	MEDIUM

205.097	205.097	$C_{11}H_{12}O_2N_2$	7	LOW
205.133	205.134	$C_{12}H_{16}ON_2$	6	MEDIUM
205.169	205.170	$C_{13}H_{20}N_2$	5	MEDIUM
206.117	206.118	$C_{12}H_{15}O_2N$	6	LOW
207.112	207.113	$C_{11}H_{14}O_2N_2$	6	LOW
207.149	207.149	$C_{12}H_{18}ON_2$	5	LOW
209.107	209.107	$C_{14}H_{12}N_2$	10	MEDIUM
209.128	209.128	$C_{11}H_{16}O_2N_2$	5	LOW
211.144	211.144	$C_{11}H_{18}O_2N_2$	4	MEDIUM
212.106	212.107	$C_{14}H_{13}ON$	9	MEDIUM
212.118	212.118	$C_{13}H_{13}N_3$	9	LOW
214.086	214.086	$C_{13}H_{11}O_2N$	9	MEDIUM
215.117	215.118	$C_{13}H_{14}ON_2$	8	MEDIUM
216.149	216.150	$C_{13}H_{17}N_3$	7	LOW
217.085	217.086	$C_{13}H_{12}O_3$	8	LOW
217.097	217.097	$C_{12}H_{12}O_2N_2$	8	MEDIUM
218.103	218.104	$C_{10}H_{11}ON_5$	8	LOW
218.117	218.118	$C_{13}H_{15}O_2N$	7	LOW
218.165	218.165	$C_{13}H_{19}N_3$	6	LOW
219.112	219.113	$C_{12}H_{14}O_2N_2$	7	MEDIUM
219.149	219.149	$C_{13}H_{18}ON_2$	6	LOW
219.185	219.186	$C_{14}H_{22}N_2$	5	MEDIUM
221.080	221.081	$C_{12}H_{12}O_4$	7	LOW
221.128	221.128	$C_{12}H_{16}O_2N_2$	6	MEDIUM
221.201	221.201	$C_{14}H_{24}N_2$	4	MEDIUM
223.122	223.123	$C_{15}H_{14}N_2$	10	MEDIUM
223.216	223.217	$C_{14}H_{26}N_2$	3	MEDIUM
224.107	224.107	$C_{15}H_{13}ON$	10	LOW
225.102	225.102	$C_{14}H_{12}ON_2$	10	MEDIUM
225.138	225.139	$C_{15}H_{16}N_2$	9	MEDIUM
226.122	226.123	$C_{15}H_{15}ON$	9	MEDIUM
227.117	227.118	$C_{14}H_{14}ON_2$	9	MEDIUM
228.101	228.102	$C_{14}H_{13}O_2N$	9	MEDIUM
228.138	228.138	$C_{15}H_{17}ON$	8	MEDIUM
230.164	230.165	$C_{14}H_{19}N_3$	7	LOW
231.112	231.113	$C_{13}H_{14}O_2N_2$	8	MEDIUM
232.133	232.133	$C_{14}H_{17}O_2N$	7	LOW

233.128	233.128	$C_{13}H_{16}O_2N_2$	7	LOW
233.164	233.165	$C_{14}H_{20}ON_2$	6	LOW
233.201	233.201	$C_{15}H_{24}N_2$	5	MEDIUM
235.216	235.217	$C_{15}H_{26}N_2$	4	MEDIUM
237.138	237.139	$C_{16}H_{16}N_2$	10	MEDIUM
239.117	239.118	$C_{15}H_{14}ON_2$	10	MEDIUM
239.153	239.154	$C_{16}H_{18}N_2$	9	MEDIUM
241.133	241.134	$C_{15}H_{16}ON_2$	9	MEDIUM
242.117	242.118	$C_{15}H_{15}O_2N$	9	LOW
243.112	243.113	$C_{14}H_{14}O_2N_2$	9	LOW
244.096	244.097	$C_{14}H_{13}O_3N$	9	LOW
245.128	245.128	$C_{14}H_{16}O_2N_2$	8	MEDIUM
245.164	245.165	$C_{15}H_{20}ON_2$	7	MEDIUM
247.143	247.144	$C_{14}H_{18}O_2N_2$	7	LOW
247.216	247.217	$C_{16}H_{26}N_2$	5	MEDIUM
249.232	249.233	$C_{16}H_{28}N_2$	4	MEDIUM
251.153	251.154	$C_{17}H_{18}N_2$	10	LOW
253.133	253.134	$C_{16}H_{16}ON_2$	10	LOW
255.112	255.113	$C_{15}H_{14}O_2N_2$	10	LOW
255.148	255.149	$C_{16}H_{18}ON_2$	9	LOW
255.185	255.186	$C_{17}H_{22}N_2$	8	LOW
258.112	258.112	$C_{15}H_{15}O_3N$	9	LOW
259.143	259.144	$C_{15}H_{18}O_2N_2$	8	LOW
259.180	259.180	$C_{16}H_{22}ON_2$	7	LOW
269.127	269.128	$C_{16}H_{16}O_2N_2$	10	LOW
283.143	283.144	$C_{17}H_{18}O_2N_2$	10	LOW

[*]species detected as an ion-radical

Table 3: The list of retention times, absorption peak maxima, and chemical formulas of the BrC chromophores detected in the brushwood smoke sample. Tentative assignments are given based on compounds previously identified in the lignin pyrolysis literature.

LC retention time (min)	λ_{max} (nm)	Nominal molecular weight (amu)	Chemical formula(s)	Tentative assignment
6.26	383	192	$C_9H_8N_2O_3$	
7.15	392	141	$C_7H_8O_3$	
10.55	305	183	$C_9H_{10}O_4$	Homovanillic acid/syringealdehyde
13.29	265	155	$C_8H_{10}O_3$	Syringol
14.44	305	169	$C_8H_8O_4$	Vanillic acid
		183	$C_9H_{10}O_4$	Homovanillic

				acid/syringealdehyde
15.57	299	181	$C_{10}H_{12}O_3$	Ethyl-3-methoxybenzoate
		167	$C_9H_{10}O_3$	Veratraldehyde
16.95	313, 334	186	$C_{11}H_7NO_2$	
17.25	331	165	$C_9H_8O_3$	
		162	$C_9H_7NO_2$	
18.13	341	209	$C_{11}H_{12}O_4$	
18.32	229, 337	179	$C_{10}H_{10}O_3$	
19.78	305, 330	194	$C_{10}H_{10}O_4$	Ferulic acid
24.11	290, 330	259	$C_{15}H_{14}O_4$	
28.07	334	184	$C_8H_9NO_4$	
29.24	330	198	$C_{13}H_{10}O_2$	
		230	$C_{13}H_{10}O_4$	
33.81	340	227	$C_{14}H_{10}O_3$	

Table 4: The list of retention times, absorption peak maxima, and chemical formulas of the BrC chromophores detected in the the dung smoke sample. Tentative assignments are given based on compounds previously identified in the lignin pyrolysis literature.

LC retention time (min)	λ_{max} (nm)	Nominal molecular weight (amu)	Chemical formula(s)	Tentative assignment
8.50	295	167	$C_8H_9NO_3$	
9.09	282,300	166	$C_9H_{10}O_3$	
		168	$C_8H_8O_4$	
10.59	252, 289, 393	182	$C_9H_{10}O_4$	Homovanillic acid/syringealdehyde
12.22	282	122	$C_7H_6O_2$	Benzoic acid
14.44	306	168	$C_8H_8O_4$	Vanillic acid
		182	$C_9H_{10}O_4$	Homovanillic acid/syringealdehyde
		164	$C_9H_8O_3$	
15.57	300	174	$C_{10}H_{12}O_3$	Ethyl-3-methoxybenzoate
		166	$C_9H_{10}O_3$	Veratraldehyde
16.35	286	174	$C_{11}H_{10}O_2$	
18.28	290, 330[a]	162	$C_{10}H_{10}O_2$	
19.5	323[a]	220	$C_{12}H_{12}O_4$	
19.72	331[a]	194	$C_{10}H_{10}O_4$	Ferulic acid
20.85	352[a]	188	$C_{12}H_{12}O_2$	
24.54	299, 308	178	$C_{10}H_{10}O_3$	
25.28	290, 320	218	$C_{12}H_{10}O_4$	
29.17	332	198	$C_{13}H_{10}O_2$	
		230	$C_{13}H_{10}O_4$	
29.60	358[a]	213	$C_{13}H_9O_3$	

[a] signifies a shoulder, rather than a clear peak